PLOS PATHOGENS

RESEARCH ARTICLE

Interactions between B cells and T follicular regulatory cells enhance susceptibility to *Brucella* infection independent of the anti-*Brucella* humoral response

Alexis S. Dadelahi[1,2¤a], Mostafa F. N. Abushahba[1,2,3], Bárbara Ponzilacqua-Silva[1,2], Catherine A. Chambers[1,2¤b], Charles R. Moley[1,2], Carolyn A. Lacey[1,2¤c], Alexander L. Dent[4], Jerod A. Skyberg[1,2]*

1 Department of Veterinary Pathobiology, College of Veterinary Medicine, University of Missouri, Columbia, Missouri, United States of America, **2** Laboratory for Infectious Disease Research, University of Missouri, Columbia, Missouri, United States of America, **3** Department of Zoonoses, Faculty of Veterinary Medicine, Assiut University, Assiut, Egypt, **4** Department of Microbiology and Immunology, Indiana University School of Medicine, Indianapolis, Indiana

¤a Current address: ARUP Institute for Clinical and Experimental Pathology, Department of Pathology, University of Utah School of Medicine, Salt Lake City, Utah, United States of America
¤b Current address: University Research Animal Resources, University of Georgia, Athens, Georgia
¤c Current address: AbbVie, Chicago, Illinois
* skybergj@missouri.edu

Citation: Dadelahi AS, Abushahba MFN, Ponzilacqua-Silva B, Chambers CA, Moley CR, Lacey CA, et al. (2023) Interactions between B cells and T follicular regulatory cells enhance susceptibility to *Brucella* infection independent of the anti-*Brucella* humoral response. PLoS Pathog 19(9): e1011672. https://doi.org/10.1371/journal.ppat.1011672

Editor: Renée M. Tsolis, University of California, Davis, UNITED STATES

Received: May 31, 2023

Accepted: September 7, 2023

Published: September 18, 2023

Data Availability Statement: The RNA-seq data discussed in this publication have been deposited in the NCBI Gene Expression Omnibus (GEO) and are accessible through GEO Series accession number GSE231772. All other data relevant data are in the manuscript and Supporting Information files.

Funding: This project has been funded in part with Federal funds from the National Institute of Allergy

Abstract

Brucellosis, caused by facultative, intracellular *Brucella* spp., often results in chronic and/or lifelong infection. Therefore, *Brucella* must employ mechanisms to subvert adaptive immunity to cause chronic infection. B lymphocytes enhance susceptibility to infection with *Brucella* spp. though the mechanisms remain unclear. Here we investigated the role of antibody secretion, B cell receptor (BCR) specificity, and B cell antigen presentation on susceptibility to *B. melitensis*. We report that mice unable to secrete antibody do not display altered resistance to *Brucella*. However, animals with B cells that are unable to recognize *Brucella* through their BCR are resistant to infection. In addition, B cell MHCII expression enhances susceptibility to infection in a $CD4^+$ T cell-dependent manner, and we found that follicular B cells are sufficient to inhibit $CD4^+$ T cell-mediated immunity against *Brucella*. B cells promote development of T follicular helper (T_{FH}) and T follicular regulatory (T_{FR}) cells during *Brucella* infection. Inhibition of B cell and $CD4^+$ T cell interaction via CD40L blockade enhances resistance to *Brucella* in a B cell dependent manner concomitant with suppression of T_{FH} and T_{FR} differentiation. Conversely, PD-1 blockade increases *Brucella* burdens in a B and $CD4^+$ T cell dependent manner while augmenting T regulatory (T_{Reg}) and T_{FR} responses. Intriguingly, T_{FR} deficiency enhances resistance to *Brucella* via a B cell dependent, but antibody independent mechanism. Collectively, these results demonstrate B cells support T_{FR} responses that promote susceptibility to *Brucella* infection independent of the antibody response.

and Infectious Diseases, National Institutes of Health, Department of Health and Human Services under grant R01AI150797 to J.S. The funders had no role in study design, data collection and analysis, decision to publish, or preparation of the manuscript.

Competing interests: I have read the journal's policy and the authors of this manuscript have the following competing interests. Carolyn Lacey is now employed by AbbVie. This article is composed of the authors' work and ideas and does not reflect the ideas of AbbVie. The remaining authors declare that the research was conducted in the absence of any commercial or financial relationships that could be construed as a potential conflict of interest.

Author summary

Brucella can cause a life-long infection in humans, mice and livestock making it an ideal organism for investigating the mechanisms that pathogens employ to subvert host immunity and cause chronic infection. Here, we determined how B cell effector functions enhance susceptibility to *Brucella*. We found that animals with B cells that are unable to recognize *Brucella* through their BCR are resistant to infection. We also found that B cells alter the function of $CD4^+$ T cells during *Brucella* infection in a MHCII- and CD40: CD40L-dependent manner. Moreover, we show that B cells promote development of T follicular regulatory cells that in turn enhance susceptibility to *Brucella* in an antibody independent manner. This was of particular interest, because to our knowledge, an antibody independent function of T follicular regulatory cells in modulating susceptibility to infection has not been previously reported. Collectively, this study highlights mechanisms by which *Brucella* infection subverts B and $CD4^+$ T cell interactions to promote host susceptibility to infection.

Introduction

Consistently ranked by the World Health Organization as one of the world's most common neglected zoonoses, brucellosis remains a major impediment to human health and economic stability [1,2]. Due to non-descript clinical signs and inadequate testing procedures, it is likely that global brucellosis incidence is grossly underestimated, and the chronicity of infection further complicates measures to mitigate disease [3,4]. Infection occurs frequently following consumption of unpasteurized dairy products or contact with tissues from livestock infected with the gram negative, facultative intracellular bacteria, *Brucella* [5–7]. Chronic disease is a frequent outcome of infection, even when aggressive antibiotic therapy is employed, and is typified by onset of various sequelae including relapsing undulant fever, arthritis, and neurobrucellosis [2,5]. Currently, our understanding of mechanisms that allow *Brucella* spp. to circumvent protective host responses are lacking and represent a major limitation for rational vaccine and therapeutic development.

IFN-γ is crucial to effective control of infection [8,9], and endogenous Th1, Th17 and $CD8^+$ T cell responses, in the right context, can confer some level of protection [2,10–15]. However, *Brucella* can cause a lifelong infection in humans, livestock, and mice [10,16,17], and robust protection (that which results in one log or greater reduction in bacterial burden) typically fails to arise prior to one-month post infection, underscoring the inefficiency of this response.

B cell deficient mice display enhanced resistance to *Brucella* that is not altered by passive transfer of antibody [10,18]. We previously reported B cells require $CD4^+$ T cells to promote susceptibility to infection, indicating that $CD4^+$ T cell and B cell interactions are detrimental to control of *Brucella* [19]. However, the nature of this interaction remains undefined. T_{FH} comprise a subset of $CD4^+$ T cells specialized in providing essential help to follicular B cells (Fo B) during the germinal center (GC) response via CD40L, IL-21 and IL-4 [20]. Efficient class switching, affinity maturation, and generation of memory and plasma B cells during infection depend upon this crucial interaction; however, tight regulation of this process is vital for prevention of self-reactivity while also facilitating control of infection [20]. The role of T_{FR} in fine-tuning this response has recently come to light. T_{FR} share many characteristics in common with T_{FH} populations including expression of Bcl6, CXCR5, ICOS, and PD-1 [21]. Additionally, T_{FR} share various characteristics with T_{Reg} including expression of FoxP3, GITR, and

CTLA-4 [22–25]. Compelling evidence points to a regulatory role for T_{FR} throughout the GC response, which includes conditioning both the magnitude and quality of the response via suppression of T_{FH} and germinal center B cells (GC B) [22–24,26–33]. While this function is likely dependent on the enhanced ability of T_{FR} to suppress B cell responses specifically [22,24,26,34], the mechanisms involved in this process are largely undefined.

Here we show both B cell receptor (BCR) specificity and B cell antigen presentation function to enhance susceptibility to *Brucella*. Fo B are sufficient for inhibition of protective $CD4^+$ T cell responses, and B cells promote T_{Reg} and T_{FR} populations which were associated with enhanced susceptibility to *Brucella*. Using T_{FR} deficient mice, we demonstrate T_{FR} enhance susceptibility to *Brucella* in a B cell-dependent, but antibody independent, manner.

Results

Role of BCR specificity and secreted antibody in uptake of *Brucella* by B cells and host susceptibility to infection

BCR-mediated antigen uptake is 100- to 1000-fold more efficient for cognate T cell activation via MHCII than BCR-independent routes of B cell antigen presentation [35]. To investigate whether BCR specificity for *Brucella* alters susceptibility to infection, we challenged WT and MD4 mice, in which ~90% of B cells express a BCR specific for the irrelevant antigen hen egg lysozyme (HEL) [36] with *B. melitensis*. Significantly fewer *Brucella* were recovered from spleens of MD4 mice by four weeks post challenge (Fig 1A). Levels of total IgG and IgM were reduced ~10-fold in MD4 mice (S1A Fig), similar to what has been observed in MD4 mice in other infection models [37]. However, MD4 animals generated ~1000-fold less anti-*Brucella*

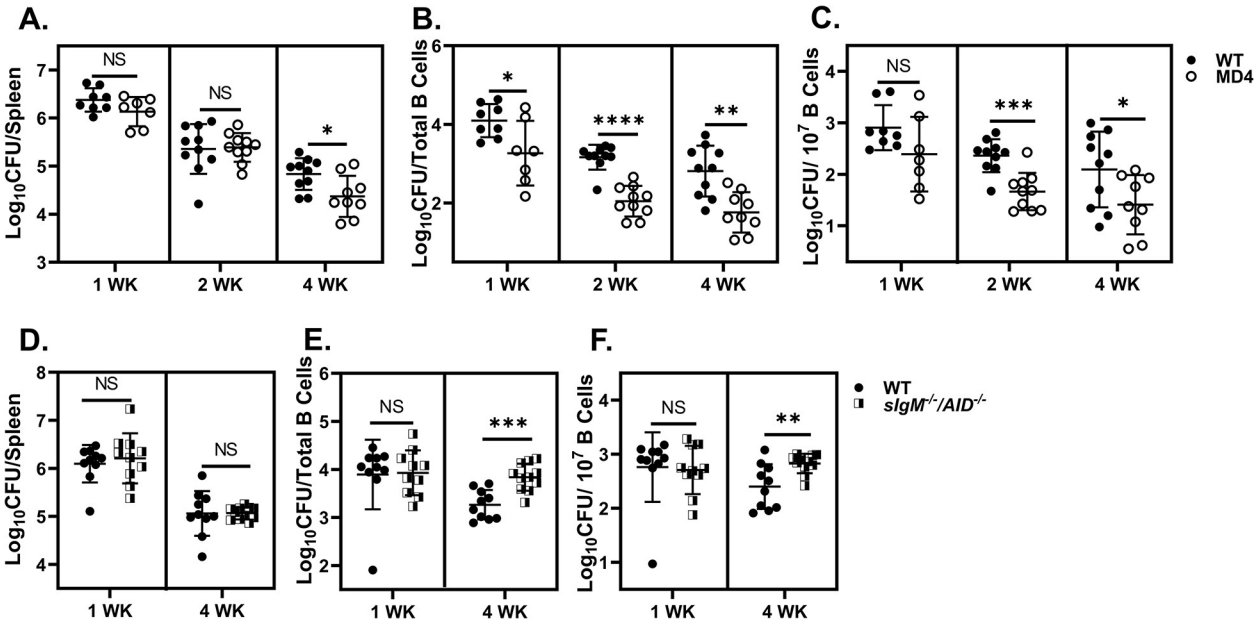

Fig 1. Role of BCR specificity and secreted antibody in susceptibility to infection and B cell uptake of *Brucella*. MD4 mice or WT littermates (n = 7-10/group/timepoint) were challenged i.p. with $1x10^5$ CFUs of *B. melitensis* 16M. **(A)** Splenic bacterial burdens measured at one-, two-, and four-weeks post infection. **(B)** Viable intracellular *Brucella* recovered from total sorted $CD19^+$ splenic B cells at one, two- and four-weeks post infection. **(C)** Viable intracellular *Brucella* burden per sorted B cell recovered at one, two- and four weeks post challenge. **(D)** Splenic bacterial loads of WT and $sIgM^{-/-}/AID^{-/-}$ mice (n = 10-12/group/timepoint) at one- and four-weeks post challenge with *B. melitensis*. **(E)** Total viable intracellular *Brucella* recovered from sorted $CD19^+$ splenic B cells at one- and four-weeks post infection in WT and $sIgM^{-/-}/AID^{-/-}$ animals. **(F)** Viable intracellular *Brucella* burden per sorted B cell recovered at one-, and four-weeks post challenge in WT and $sIgM^{-/-}/AID^{-/-}$ mice. **(A-F)** Data are combined from 2 independent experiments per time point.

https://doi.org/10.1371/journal.ppat.1011672.g001

IgG compared to WT controls at both two- and four-weeks post infection (S1B and S1C Fig), confirming a reduced affinity for *Brucella* antigen by MD4 B cells. Taken together, these results suggest that BCR specificity for *Brucella* promotes susceptibility to infection.

Because B cell uptake of antigen is more efficient via the BCR than alternate mechanisms [35], we investigated the impact of BCR specificity on *Brucella* uptake by B lymphocytes. Compared to WT controls, B cell lysates collected from MD4 mice consistently harbored fewer *Brucella* with ~10-fold reduction at one-, two-, and four-weeks post challenge (Fig 1B). MD4 and WT mice harbor similar levels of splenic *B. melitensis* through the first two weeks of infection (Fig 1A) indicating that reduced B cell uptake of *Brucella* is a B cell specific effect rather than a result of diminished total bacterial burden in MD4 animals. Because we recovered fewer B cells from MD4 animals relative to WT mice (S1D Fig), we calculated the number of *B. melitensis* CFUs recovered per B cell and found this was also significantly reduced at two- and four-weeks post infection in MD4 animals (Fig 1C). Collectively, these data indicate that a diminished capacity for BCR-mediated recognition of *Brucella* impairs uptake of *Brucella* by B cells, which in turn may alter host susceptibility to infection.

Opsonization of *Brucella* with IgM from previously infected mice enhances uptake by B cells *in vitro* [4]. To investigate the effect of *Brucella*-specific antibody on uptake *in vivo* we employed $sIgM^{-/-}/AID^{-/-}$ mice which express a polyclonal BCR but do not secrete IgM nor generate class-switched antibodies [38]. Total splenic *Brucella* burdens were similar among WT and $sIgM^{-/-}/AID^{-/-}$ animals at both one- and four-weeks post-infection (Fig 1D). In contrast to MD4 mice (Fig 1B), $sIgM^{-/-}/AID^{-/-}$ mice displayed similar intracellular *Brucella* B cell burdens one week post infection and increased B cell burdens at four weeks post infection relative to WT mice (Fig 1E and 1F). These data indicate that secreted antibody does not alter susceptibility to infection, nor is it absolutely required for *Brucella* entry into B cells.

B cell antigen presentation promotes deleterious CD4$^+$ T cell responses

BCR-mediated antigen uptake, trafficking and presentation are regulated by Bruton's tyrosine kinase (Btk) [39]. Therefore, we infected mice with a mutational defect in Btk (XID) and compared control of infection to CBA/J control mice. Bacterial burdens were similar two weeks post infection, but XID mice displayed enhanced resistance by four weeks post challenge (Fig 2A) suggesting Btk-dependent B cell antigen presentation enhances susceptibility to brucellosis. In addition to disrupting BCR-mediated antigen presentation, Btk dysfunction

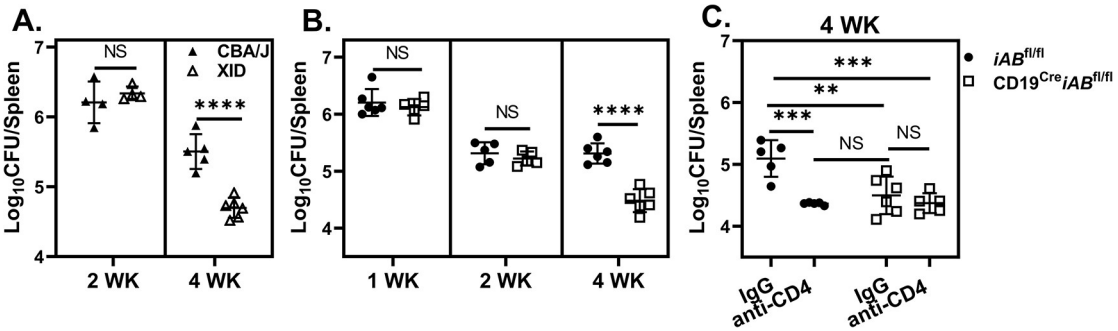

Fig 2. B cell antigen presentation promotes deleterious CD4$^+$ T cell responses during *Brucella* infection. (A) Splenic *Brucella* loads of XID and CBA/J animals (n = 4-6/group/timepoint) following challenge with *B. melitensis* at two- and four-weeks post infection. **(B)** Splenic *Brucella* burden of $CD19^{Cre}iAB^{fl/fl}$ or $iAB^{fl/fl}$ littermates (n = 3-7/group/timepoint) at one-, two-, and four-weeks post infection. **(C)** $CD19^{Cre}iAB^{fl/fl}$ and $iAB^{fl/fl}$ mice were treated with CD4$^+$ T cell-depleting antibody, or IgG isotype, and challenged with *B. melitensis*. Four weeks post infection splenic *Brucella* burdens were compared. Data are representative of at least two independent experiments.

https://doi.org/10.1371/journal.ppat.1011672.g002

suppresses B-1a cell development in XID mice [40] which can impact control of infection [41]. However adoptive transfer of B-1a cells from naive CBA/J donors to XID mice prior to challenge did not alter control of *Brucella* (S1E Fig), indicating resistance in XID animals is independent of B-1a cell deficiency.

To further examine the role of B cell antigen presentation on $CD4^+$ T cell responses to *Brucella*, we compared control of infection in B cell specific MHCII deficient mice ($CD19^{Cre}iAB^{fl/fl}$) and $iAB^{fl/fl}$ control animals and found B cell specific MHCII deficiency enhanced resistance to *Brucella* four weeks post infection (Fig 2B). Additionally, while depletion of $CD4^+$ T cells from $iAB^{fl/fl}$ mice enhanced resistance to infection, $CD4^+$ T cell depletion had no effect in $CD19^{Cre}iAB^{fl/fl}$ mice at four weeks post infection (Fig 2C). This indicated that B cell MHCII expression promotes $CD4^+$ T cell responses that enhance susceptibility to *Brucella*.

Follicular B cells Promote Susceptibility to *Brucella*

We next compared $CD4^+$ T cell phenotypes in B cell deficient (μMT) and WT mice infected with *B. melitensis*. At one week post infection, we observed a significant increase in the percentage of activated ($CD44^+$) $CD4^+$ T cells in μMT mice (Fig 3A). μMT mice also displayed ~30% increase in T-bet expression on $CD44^+CD4^+$ T cells one week post infection, though this difference dissipated two weeks post challenge (Figs 3B and S1F). FoxP3 expression on $CD44^+CD4^+$ T cells was significantly decreased among μMT animals compared to WT at one- and two weeks post infection (Figs 3C and S1G), suggesting B cells may drive T_{Reg} differentiation in response to *Brucella*. Because μMT mice can exhibit altered T cell development [42], we confirmed our findings with adoptive transfer experiments. $Rag1^{-/-}$ animals received $CD4^+$ T cells alone, or both $CD4^+$ T and B cells from WT donors prior to challenge with *B. melitensis*. Similar to our findings in μMT mice, by two weeks post infection co-transfer of B cells enhanced FoxP3 expression and diminished T-bet expression on $CD44^+CD4^+$ T cells (S1H and S1I Fig).

Further analysis of $CD44^+CD4^+$ T cells in WT animals revealed FoxP3 expression was preferentially enhanced among $CXCR5^+$ populations vs $CXCR5^-$ populations (15.40% ±1.93% vs 3.6 ±1.22) at two- and four-weeks post infection (Fig 3D). WT mice also display increased $FoxP3^+$ cell frequencies amongst $CXCR5^+CD44^+CD4^+$ T cell populations one week post infection compared to μMT animals (Fig 3E), suggesting B cells promote T_{Reg} development amongst $CXCR5^+CD44^+CD4^+$ T cells during *Brucella* infection.

CXCR5 expression facilitates $CD4^+$ T cell trafficking to B cell follicles and subsequent interaction with cognate Fo B [43–45]. To test the role of Fo B during *Brucella* infection, we adoptively transferred $CD4^+$ T cells alone, or both $CD4^+$ T cells and Fo B into $Rag1^{-/-}$ mice prior to challenge. At four weeks post infection, co-transfer of Fo B with $CD4^+$ T cells resulted in ~10-fold increase in splenic *Brucella* loads compared to animals transferred $CD4^+$ T cells alone (Fig 3F), demonstrating Fo B inhibit $CD4^+$ T cell responses following *B. melitensis* infection. Notably, we observed no marked effect in adoptive transfer experiments in which B-1a cells were co-transferred with $CD4^+$ T cells (S1J Fig).

CD40L blockade enhances resistance to *Brucella*

CD40:CD40L interactions between T_{FH}, and Fo B following priming are requisite for generation of GC responses [46,47]. Thus, we hypothesized inhibition of CD40:CD40L interactions could suppress the deleterious effects resulting from interaction of $CD4^+$ T cells and Fo B during *Brucella* infection. Interestingly, CD40L blockade in WT, but not uMT animals, enhanced control of splenic *Brucella* burdens four weeks post infection (Fig 4A and 4B), indicating the deleterious effect of CD40:CD40L interactions is B cell dependent. CD40L

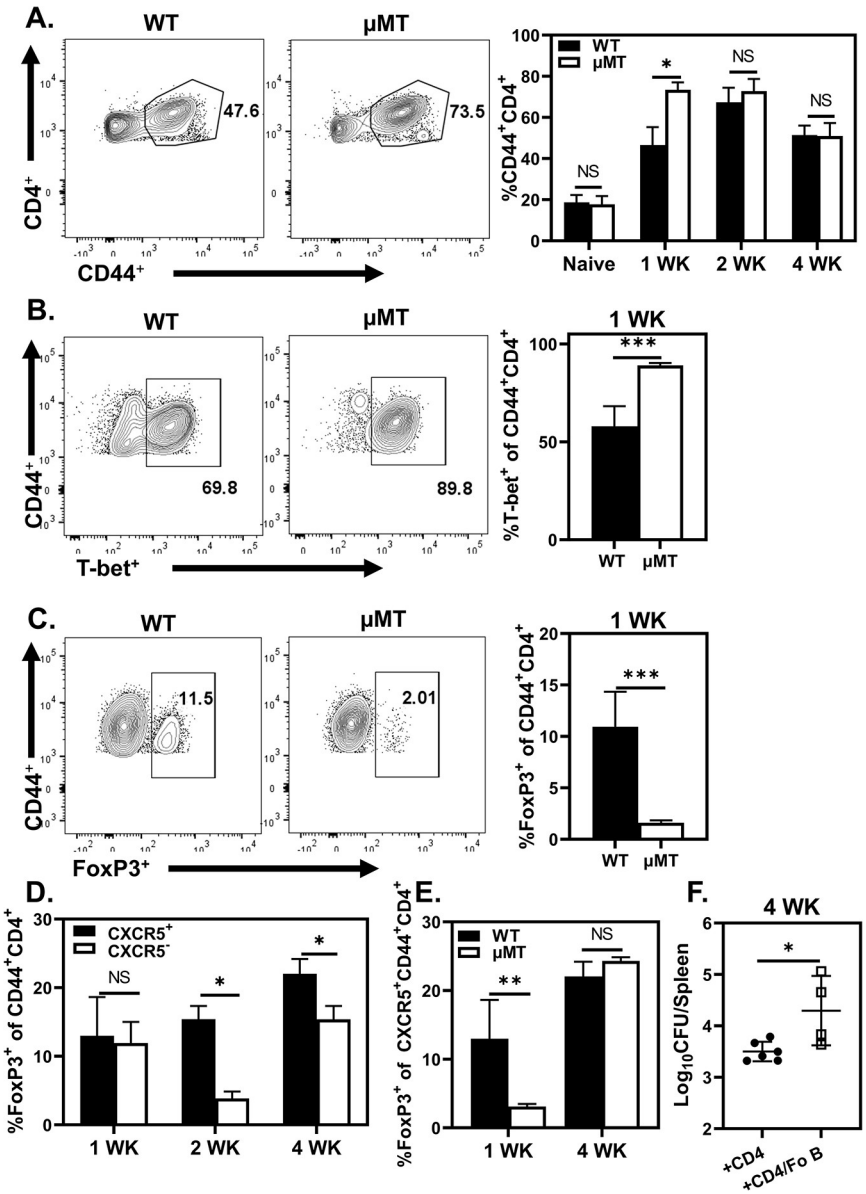

Fig 3. Fo B inhibit CD4$^+$ T cell immunity to *Brucella*. Splenic CD4$^+$ T cell responses assessed via flow cytometry in naïve (n = 2) or *B. melitensis* infected WT and μMT mice (n = 3-6/group/time point) at one-, or four-weeks post infection. Quantification of CD44 expression on CD4$^+$ T cells **(A)** along with T-bet **(B)**, and FoxP3 **(C)** expression on CD44 expressing CD4$^+$ T cells**. (D)** Proportion of FoxP3$^+$ cells among CXCR5$^+$ and CXCR5$^-$ CD44$^+$CD4$^+$ T cells at one-, two-, and four-weeks post infection in WT animals. **(E)** Proportion of FoxP3$^+$ cells amongst CXCR5$^+$CD44$^+$CD4$^+$ T cells in WT and μMT mice one- and four-weeks post infection. **(F)** *Rag1*$^{-/-}$ mice (n = 3-7/treatment) adoptively transferred either CD4$^+$ T cells alone, or CD4$^+$ T cells in combination with purified Fo B cells one day prior to *B. melitensis* challenge. Data are representative of at least two independent experiments.

https://doi.org/10.1371/journal.ppat.1011672.g003

blockade also suppressed GC B cell responses (Figs 4C, 4D, S2A and S2B) and the proportion of T_{Reg}, T_{FH}, and T_{FR} four-weeks post challenge (Figs 4E–4H and S2C–S2E). Collectively these data establish that interruption of CD40:CD40L interactions enhances resistance to *Brucella*, and suggest disrupting GC B, T_{Reg}, T_{FH}, and/or T_{FR} populations may improve control of infection.

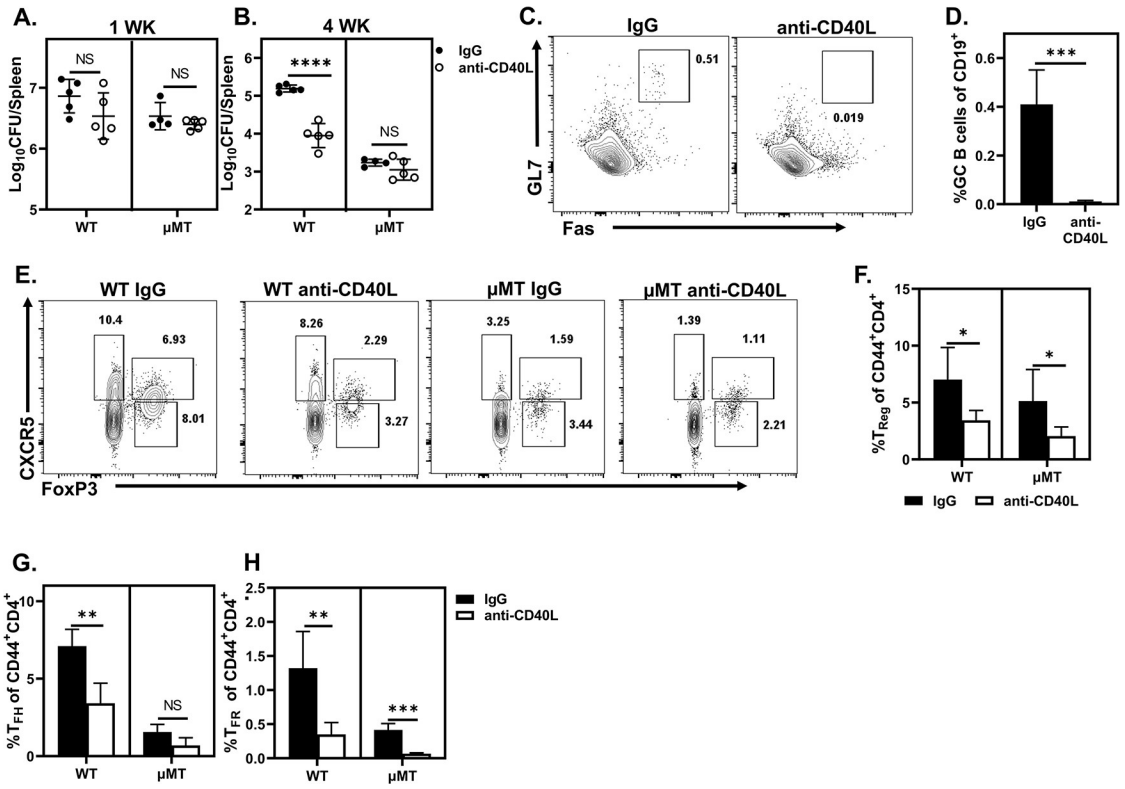

Fig 4. CD40L blockade enhances resistance to *Brucella*. **(A-H)** Mice (n = 3-5/group) were treated with CD40L blocking antibody or IgG. **(A-B)** Splenic *Brucella* burdens were measured in WT and μMT mice one **(A)** and four **(B)** weeks post infection. Representative plots **(C)** and quantification **(D)** of the percentage of GC B cells ($CD19^+CD43^-GL7^+Fas^+$) among $CD19^+$ B cells in isotype or anti-CD40L treated WT animals. **(E-G)** Representative plots showing CXCR5 and FoxP3 expression **(E)** and quantification **(F-H)** of the percentage of T_{Reg} ($FoxP3^+CXCR5^-$) **(F)**, T_{FH} ($FoxP3^-ICOS^+CXCR5^+$) **(G)**, and T_{FR} ($FoxP3^+ICOS^+CXCR5^+$) **(H)** amongst $CD44^+CD4^+$ T cells in IgG and anti-CD40L-treated WT and μMT mice four weeks post infection. Data are representative of at least two independent experiments.

https://doi.org/10.1371/journal.ppat.1011672.g004

Bcl6 expression in CD4 T cells protects the host against *Brucella*

Expression of Bcl6 in $CD4^+$ T cells is essential to differentiation of both T_{FH} and T_{FR} [22,48,49]. To ascertain whether *Brucella* infection is exacerbated by B cell interaction with Bcl6 expressing $CD4^+$ T cells, we infected $CD4^{Cre}Bcl6^{fl/fl}$ mice with *B. melitensis*. While depletion of total $CD4^+$ T cells enhances resistance (Fig 2C), deletion of $Bcl6^+CD4^+$ T cells increased susceptibility to *Brucella* four weeks post challenge (Fig 5A). Thymocytes express both CD8 and CD4 during early development, and Bcl6 is expressed by some splenic $CD8^+$ T cells [50,51]. However, we found enhanced susceptibility in $CD4^{Cre}Bcl6^{fl/fl}$ mice did not require $CD8^+$ T cells (S2F Fig). Similar to previous reports [25,52], deletion of Bcl6 in $CD4^+$ T cells suppressed differentiation of GC B cells, T_{FH}, and T_{FR}, though T-bet expression remained similar between groups (Figs 5B–5F and S2G). While $CD4^{Cre}Bcl6^{fl/fl}$ mice had markedly reduced levels of GC B cells (Fig 5B and 5C), B cell depleted $CD4^{Cre}Bcl6^{fl/fl}$ animals displayed ~100-fold decrease in splenic *Brucella* loads compared to controls (Fig 5I) suggesting GC B cells are not essential for B cell mediated susceptibility to *Brucella*. We also observed a marked increase in both the frequency and absolute number of T_{Reg} following *Brucella* infection in $CD4^{Cre}Bcl6^{fl/fl}$ animals (Figs 5G, 5H and S2H). This was of interest given that CD40L blockade, which results in protection associated with suppression of T_{FH}, T_{FR} and GC B, significantly reduced T_{Reg} frequencies (Fig 4F–4H). Taken together, these findings suggest one or more Bcl6 expressing

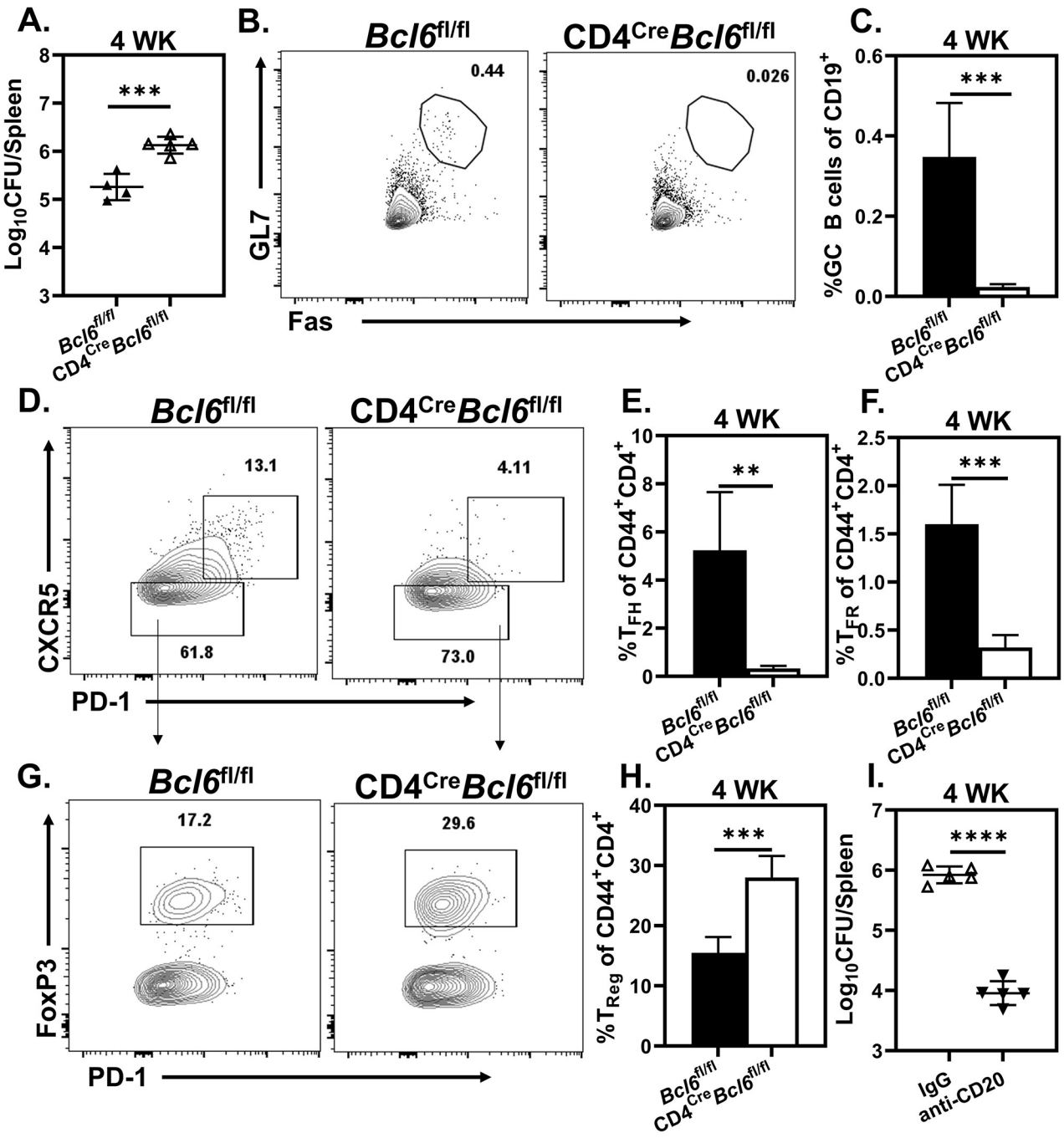

Fig 5. Lack of Bcl6 expressing CD4$^+$ T cells impairs protection against *Brucella*. *Bcl6*$^{fl/fl}$ or CD4^{Cre}*Bcl6*$^{fl/fl}$ mice (n = 4-5/group) were challenged with *B. melitensis*. **(A)** Splenic bacterial burdens measured four weeks post infection. **(B-C)** Representative plots **(B)** and quantification **(C)** of the percentage of GC B cells amongst CD19$^+$ cells four weeks post infection. **(D-F)** Representative plots showing CXCR5 and PD-1 expression **(D)** and quantification of the percent of T_{FH} (FoxP3$^-$PD-1$^+$CXCR5$^+$) **(E)** and T_{FR} (FoxP3$^+$PD-1$^+$CXCR5$^+$) **(F)** amongst CD44 expressing CD4$^+$ T cells four weeks post infection. **(G-H)** Representative plots showing FoxP3 and PD-1 expression **(G)** and quantification **(H)** of the percentage of T_{Reg} (FoxP3$^+$CXCR5$^-$) among CD44 expressing CD4$^+$ T cells four weeks post infection. **(I)** Splenic bacterial burdens of CD4^{Cre}*Bcl6*$^{fl/fl}$ animals (n = 5/treatment) treated with anti-CD20 or IgG four weeks post *Brucella* challenge. Data are representative of at least two independent experiments.

https://doi.org/10.1371/journal.ppat.1011672.g005

$CD4^+$ T cell populations may be necessary for efficient control of infection, or that outgrowth of T_{Reg} in $CD4^{Cre}Bcl6^{fl/fl}$ mice drives enhanced susceptibility to challenge.

PD-1 blockade enhances susceptibility to *Brucella*

CD40L blockade and $Bcl6^+CD4^+$ T cell deficiency both dampen T_{FH} responses yet have opposing effects on control of infection (Figs 4 and 5). Combined with our finding that B cells promote FoxP3 expression amongst $CXCR5^+CD44^+CD4^+$ T cells, we questioned whether altering T_{Reg} and T_{FR} frequencies would alter control of *Brucella*. PD-1 regulates both T_{Reg} and T_{FR} differentiation and function [27,53,54]. Intriguingly, anti-PD-1 treated WT animals exhibited significantly increased bacterial loads compared to controls four weeks post *Brucella* challenge (Fig 6A). While PD-1 expression is a key trait of T_{FH} [27,55,56], various cell populations signal through PD-1 [57]. However, neither PD-1 blocked $CD4^+$ T cell-depleted mice nor μMT animals had exacerbated infection (Fig 6B and 6C), demonstrating this effect is both $CD4^+$T and B cell dependent. PD-1 blockade enhanced T_{FH}, T_{Reg} and T_{FR} proportions during infection in WT animals, while these populations remained unchanged in anti-PD-1 treated μMT animals (Fig 6D–6G). Therefore, one or more of these populations may drive B cell-dependent susceptibility to *Brucella* infection.

B cells are not absolutely required for T_{Reg}- mediated susceptibility to *Brucella*

As PD-1 blockade enhances susceptibility to infection as well as T_{Reg} and T_{FR} outgrowth (Fig 6A, 6F and 6G), we investigated the contribution of T_{Reg} to control of infection. DEREG mice bear a diphtheria toxin receptor transgene under the control of the Foxp3 promoter, allowing for depletion of FoxP3 expressing cells by administration of diphtheria toxin (DTX). Because efficient $FoxP3^+$ cell depletion is short-lived [58,59], we treated DEREG and WT groups with (DTX) on days 14 and 15 post challenge and confirmed FoxP3 expressing $CD4^+$ T cells were diminished (S3A Fig). In line with previous reports suggesting T_{Reg} cells inhibit control of brucellosis [60,61], T_{Reg} depletion significantly enhanced resistance to *Brucella* at four weeks post-infection (S3B Fig). DTX-treated DEREG mice also presented with a decreased frequency of B cells compared to DTX-treated WT animals (S3C and S3D Fig); however, GC B and T_{FH} proportions were increased in DTX treated DEREG animals compared to WT controls (S3E, S3F,S3I and S3K Fig). T-bet expressing $CD4^+$ T effector levels were similar among FoxP3-depleted and WT groups (S3G Fig). While B cells enhance the proportion of T_{Reg} during *Brucella* infection (Figs 3C, 3E, S1G and S1H), depletion of T_{Reg} in both control and B cell depleted mice enhanced resistance to infection (S3B and S3H Fig) indicating the deleterious effect of T_{Reg} is not entirely B cell dependent.

T_{FR} enhance susceptibility to *Brucella* infection in a B cell dependent, but antibody independent, manner

DTX treatment leads to T_{FR} deficiency in DEREG mice (S3J Fig) making it unclear whether T_{Reg}, T_{FR} or both contribute to enhanced susceptibility to *Brucella*. Therefore, we employed $FoxP3^{Cre}Bcl6^{fl/fl}$ mice, in which T_{FR} are deficient while $T_{Reg,}$ $T_{FH,}$ and GC B cells remain intact [29] and found T_{FR} deficiency enhanced resistance to *Brucella* four weeks post infection (Fig 7A and 7F). $FoxP3^{Cre}Bcl6^{fl/fl}$ mice displayed elevated total T_{Reg} frequencies compared to $Bcl6^{fl/fl}$ mice (Fig 7B), though this did not adversely affect control of infection. To determine whether T_{FR} require B cells to enhance susceptibility to infection, we depleted B cells from $FoxP3^{Cre}Bcl6^{fl/fl}$ and $Bcl6^{fl/fl}$ mice. While isotype treated $FoxP3^{Cre}Bcl6^{fl/fl}$ mice were more

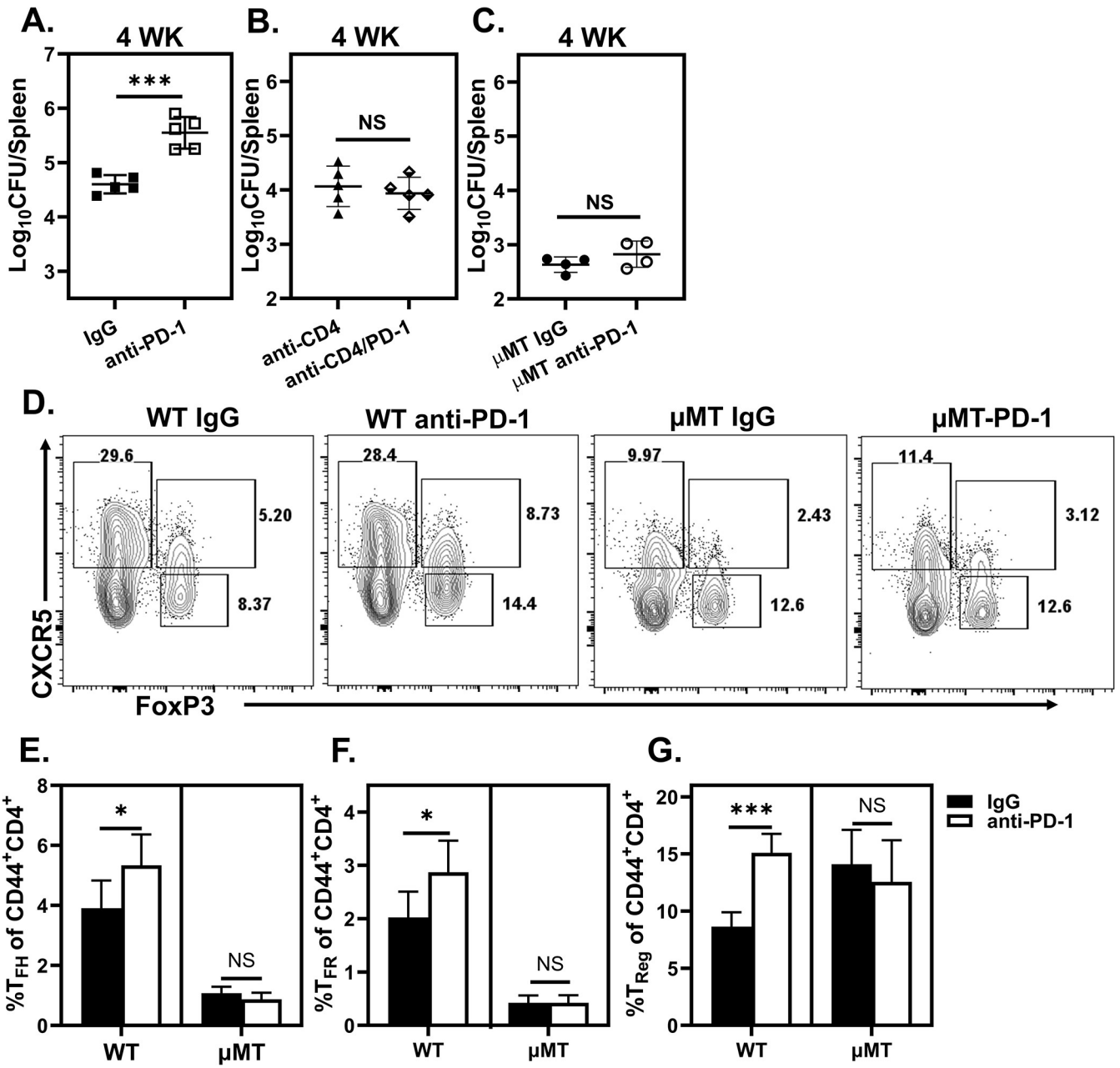

Fig 6. PD-1 blockade enhances susceptibility to *Brucella*. WT and/or μMT mice (n = 4-5/treatment) were treated with PD-1 blocking antibody, $CD4^+$ T cell depleting antibody, PD-1 blocking and CD4-depleting antibody, or isotype control. **(A & C)** Splenic bacterial loads in IgG and PD-1 blocked WT **(A)** or μMT **(C)** mice. **(B)** Splenic bacterial burden of CD4-depleted and CD4-depleted/PD-1 blocked WT mice. **(D)** Representative flow plots showing CXCR5 and FoxP3 expression and the percentage of T_{FH} ($FoxP3^-ICOS^+CXCR5^+$) **(E)**, T_{FR} ($FoxP3^+ICOS^+CXCR5^+$) **(F)**, and T_{Reg} ($FoxP3^+CXCR5^-$) **(G)** present in IgG and anti-PD-1 treated WT and μMT mice spleens four weeks post challenge. **(E-G)** Quantification of the percentage of each indicated population of CD44 expressing $CD4^+$ T cells four weeks post challenge. Data are representative of at least two independent experiments.

https://doi.org/10.1371/journal.ppat.1011672.g006

resistant to infection than isotype treated $Bcl6^{fl/fl}$ animals, *Brucella* burdens four weeks post infection were similar in $FoxP3^{Cre}Bcl6^{fl/fl}$ and $Bcl6^{fl/fl}$ mice depleted of B cells (Fig 7F). Thus, our results demonstrate that, in the absence of B cells, T_{FR} are no longer deleterious to control of infection.

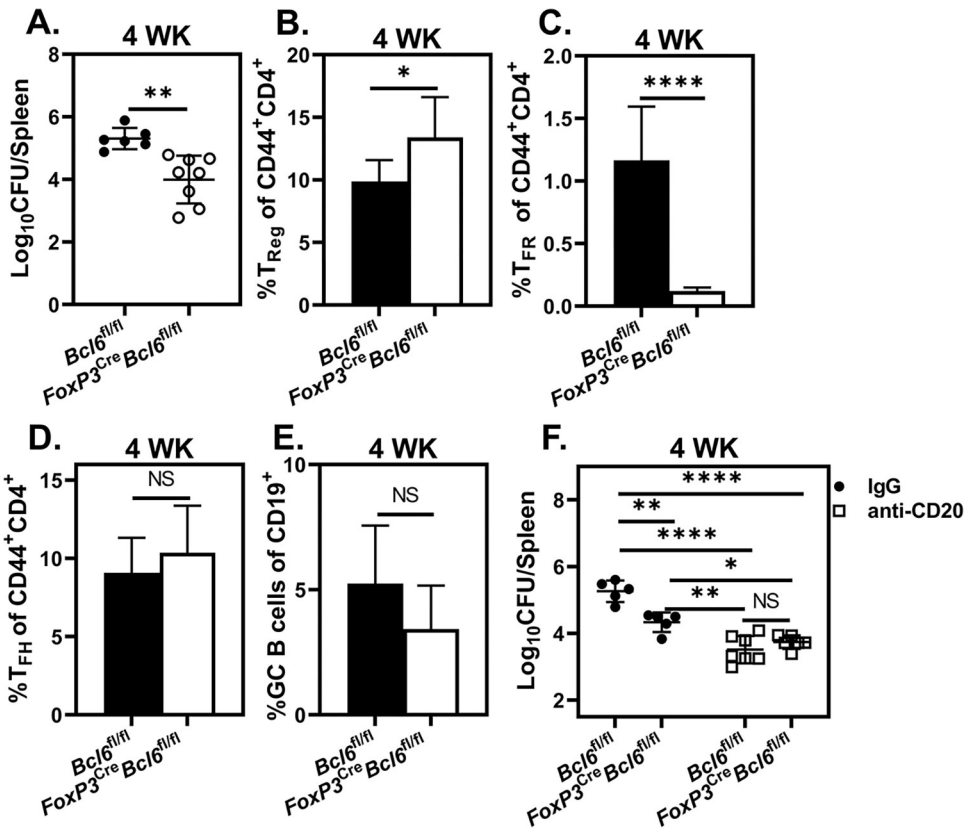

Fig 7. T_{FR} enhance susceptibility to *Brucella*. **(A)** Splenic *Brucella* burdens of *Bcl6*$^{fl/fl}$ and *FoxP3*^{Cre}*Bcl6*$^{fl/fl}$ mice (n = 5-8/group) challenged with *B. melitensis* four weeks post challenge. **(B-D)** Quantification of the mean percentage of T_{Reg} (FoxP3$^+$CXCR5$^-$) **(B)**, T_{FR} (FoxP3$^+$PD-1$^+$CXCR5$^+$) **(C)**, and T_{FH} (FoxP3$^-$PD-1$^+$CXCR5$^+$) **(D)** of CD44 expressing CD4$^+$ T cells in the spleen of infected animals four weeks post challenge. **(E)** Percentage of splenic GC B cells (Fas$^+$GL7$^+$ of CD19$^+$) amongst CD19$^+$ B cells four weeks post infection. **(F)** Splenic bacterial burdens of IgG or anti-CD20-treated *Bcl6*$^{fl/fl}$ or *FoxP3*^{Cre}*Bcl6*$^{fl/fl}$ mice (n = 4-7/treatment) four weeks after challenge with *B. melitensis*. Data are representative of at least two independent experiments.

https://doi.org/10.1371/journal.ppat.1011672.g007

As T_{FR} regulate antibody responses [28,62,63], we questioned whether T_{FR} deficiency altered antibody responses which could in turn impact control of *Brucella*. While we did not find a difference in the quantity of *Brucella*-specific IgM generated by *Bcl6*$^{fl/fl}$ and FoxP3^{Cre}*Bcl6*$^{fl/fl}$ mice four weeks post infection, FoxP3^{Cre}*Bcl6*$^{fl/fl}$ animals did display reduced anti-*Brucella* IgG levels (S4A Fig). However, passive transfer of sera from either *Bcl6*$^{fl/fl}$ or FoxP3^{Cre}*Bcl6*$^{fl/fl}$ mice previously infected with *B. melitensis* conferred similar levels of protection to FoxP3^{Cre}*Bcl6*$^{fl/fl}$ mice (S4B Fig). Coupled with our finding that control of infection is not altered in mice lacking the ability to secrete antibody (Fig 1D), these data indicate the deleterious effect of T_{FR} is independent of antibody regulatory function.

Discussion

We previously reported B cell mediated susceptibility to *Brucella* is CD4$^+$ T cell dependent [19]. Here we report that an inability of B cells to recognize *Brucella* via BCR specificity results in host resistance to infection and reduced B cell uptake of *Brucella in vivo*. While B cells enhance expression of FoxP3 and decrease expression of CD44 and T-bet by CD4$^+$ T cells in the first two weeks after infection (Figs 3A–3C and S1G), we found expression of CD44, T-bet, and FoxP3 was similar in CD4$^+$ T cells from WT and MD4 mice at one- and two-weeks post-

infection (S5A–S5F Fig). Total B cell deficiency results in a ~100-fold decrease in CFUs at 4 weeks post-infection (Figs 4B and 7F), while *Brucella* counts were reduced less than 10-fold in MD4 mice at the same timepoint (Fig 1A). The difference in phenotypes observed in MD4 mice versus mice with a total B cell deficiency could be explained by several factors. While ~90% of B cells in MD4 mice express a BCR specific for HEL [36], we did detect some *Brucella*-specific Ig MD4 mice (S1B and S1C Fig). Therefore, this residual population of non-HEL specific B cells in MD4 animals could potentially recognize *Brucella* through their BCR resulting in the dampened phenotype observed. Alternatively, while less efficient than antigen specific mechanisms, *Brucella* uptake and antigen presentation by B cells could also occur via BCR-independent processes [35].

Others have reported opsonization of *B. abortus* with IgM improves B cell uptake of bacteria *in vitro* [4]. However, we found the presence of *Brucella* specific antibody *in vivo* did not alter resistance to infection or reduce B cell *Brucella* burden (Fig 1D–1F). Interestingly, at later timepoints we found greater numbers of *Brucella* in B cells from $sIgM^{-/-}/AID^{-/-}$ mice (Fig 1E and 1F). B cells from mice that lack the ability to secrete IgM can have increased BCR signaling including elevated Btk activation [64]. This was of interest, as uptake of *Brucella* by B cells appears to be BCR specific (Fig 1), Btk is required for BCR-mediated antigen internalization [39], and because we found Btk deficiency enhances resistance to *Brucella* (Fig 2). Therefore, it is possible that enhanced BCR signaling in $sIgM^{-/-}/AID^{-/-}$ mice leads to increased uptake of *Brucella* by B cells. Alternatively, we found both the proportion and absolute number of B-1 cells in $sIgM^{-/-}/AID^{-/-}$ mice was increased >2.5 fold (S6A–S6H Fig), which is similar to what others have reported in $sIgM^{-/-}/AID^{-/-}$ mice [38]. As some B-1 cells can have phagocytic activity [65], the increased number of B-1 cells in $sIgM^{-/-}/AID^{-/-}$ mice could potentially lead to higher levels of *Brucella* within the B cell compartment.

Brucella burdens in the spleens of mice lacking B cell MHCII expression are ~10 fold lower than in control animals (Fig 2B), which is a lesser phenotype than the ~100-fold decrease in *Brucella* in mice depleted of B cells (Fig 7F) or in mice with a genetic B cell deficiency (Fig 4B). In the first week after infection, FoxP3 expression is lower while T-bet expression is higher on activated $CD4^+$ T cells in μMT mice (Fig 3B and 3C); however, we found expression of FoxP3 and T-bet was similar in activated $CD4^+$ T cells from B cell MHCII deficient mice and control animals one week post-infection (S7A–S7C Fig). In a previous study, we found increased levels of IFN-γ, TNF-α, IL-17, and IL-1β in the spleens of μMT mice at two weeks post-infection [19]. However, the levels of IFN-γ, TNF-α, IL-17, and IL-1β were similar in spleens of control and B cell MHCII deficient mice two weeks post-infection (S7D–S7I Fig). While $CD19^{Cre}$ deletes the majority of MHCII expression on B cells in $CD19^{Cre}iAB^{fl/fl}$ mice, a fraction of B cells retains B cell MHCII expression, and the proportion of $MHCII^+$ B cells in $CD19^{Cre}iAB^{fl/fl}$ mice increases over the course of infection from ~7% to ~25% (S8A Fig). Moreover, we observed a correlation between B cell MHCII expression and susceptibility to infection in $CD19^{Cre}iAB^{fl/fl}$ mice treated with IgG, but not in $CD19^{Cre}iAB^{fl/fl}$ mice depleted of $CD4^+$ T cells (S8B and S8C Fig). Therefore, the potential/capacity for residual B cell MHCII expression and subsequent $CD4^+$ T cell interaction following *Brucella* challenge in $CD19^{Cre}iAB^{fl/fl}$ mice could contribute to the diminished magnitude of the phenotype observed in these animals relative to total B cell deficiency.

Cotransfer of Fo B with $CD4^+$ T cells inhibited the ability of $CD4^+$ T cells to protect against infection (Fig 3F). Following initial antigen encounter, Fo B and T lymphocytes that have migrated to the B:T border reciprocally regulate the activation and differentiation of one another. This process relies on both B cell mediated antigen presentation and CD40:CD40L engagement [55]. Strikingly, CD40L blockade conferred protection against *Brucella* infection in WT, but not B cell deficient animals (Fig 4B). Similar to other reports [66], CD40L blockade

suppressed $T_{FH,}$ T_{FR} and GC B cell responses, signaling the GC response was ablated in treated animals (Figs 4C–4H and S2B–S2E). This suggests CD40L blockade hinders $CD4^+$ T and Fo B CD40L:CD40 engagement during *Brucella* infection. Deletion of *Bcl6* in $CD4^+$ T cells and CD40L blockade both thwart development of GC responses in *Brucella* infected mice yet have opposing effects on control of infection (Figs 4 and 5). CD40L blockade results in a decrease in the proportion of T_{Reg} (Fig 4F), while we observed that deficiency of *Bcl6* in $CD4^+$ T cells results in an increase in the proportion and absolute number of T_{Reg} following *Brucella* infection (Figs 5H and S2H). Given that T_{FR} derive from thymic and/or peripheral T_{Reg} [22,24,26,67], the increase in T_{Reg} in $CD4^{Cre}Bcl6^{fl/f}$ mice during *Brucella* infection may arise from the inability of peripheral T_{Reg} to commit to T_{FR} differentiation in response to infection. *Bcl6* restrains $CD4^+$ T cell IL-10 production [52], and $T_{Reg,}$ along with other $CD4^+$ T cell subsets, can produce IL-10 [68] which in turn promotes susceptibility of *Brucella* [69]. In particular, $CD4^+$ T cell derived IL-10 diminishes TNF-α levels during *Brucella* infection [69], and we found *Bcl6* deficiency in $CD4^+$ T cells markedly reduced TNF-α levels in the spleens of *Brucella*-infected mice (S9 Fig). Therefore, it is possible that an outgrowth of T_{Reg} and/or enhanced $CD4^+$ T cell IL-10 production in $CD4^{Cre}Bcl6^{fl/fl}$ mice results in elevated susceptibility to *Brucella*, though this would require additional investigation to confirm.

Upon depletion of B cells from $CD4^{Cre}Bcl6^{fl/f}$ mice we observed a ~100-fold decrease in splenic bacterial burdens despite the absence of GC B cells in these animals (Fig 5B, 5C and 5I). This is of interest as it suggests GC B cells are not absolutely required for B cells to mediate enhanced susceptibility and implicates early $CD4^+$ T and Fo B interactions as determinants of enhanced susceptibility to infection rather than interactions between fully committed T_{FH} and GC B cells in the GC.

PD-1 has been studied extensively in the context of chronic infection, particularly regarding its role in T cell exhaustion [57]. T cell responses to *Brucella* are inefficient at controlling infection, and $CD8^+$ T cell exhaustion is associated with chronic disease in a murine model of brucellosis [11]. Intriguingly, we found PD-1 blockade enhanced susceptibility to infection in a $CD4^+$ T and B cell-dependent manner (Fig 6A–6C). PD-1 restrains T_{Reg} and T_{FR} function [27,53,54] and upregulation of PD-1 by T_{FH} and T_{FR} contributes to follicular migration and positioning in the developing GC response [70]. Here PD-1 blockade enhanced susceptibility to *Brucella* and augmented $T_{Reg,}$ and T_{FR} populations (Fig 6F and 6G). Notably, tumor infiltrating T_{FR} are prevalent in several types of cancer, and PD-1 blockade enhances tumor-infiltrating T_{FR} leading to reduced tumor control in mice [54]. Collectively, these findings support a link between PD-1 blockade and promotion of T_{Reg} and T_{FR} which may directly impact host susceptibility to infection and the efficiency of tumor control.

Alterations in T_{Reg} and T_{FR} frequencies induced by PD-1 blockade were B cell dependent (Fig 6F and 6G). B cell expression of PD-L1 is implicated in T_{FH} differentiation and migration [71], and PD-L1 expression by B cells has been linked to B cell regulatory function which can inhibit $CD4^+$ T cell responses [72]. Interestingly, antigen-specific B cells protect against *Mycobacterium tuberculosis* infection, specifically through PD-L1 expressing B cells engaging $PD\text{-}1^+$ T_{FH}-like cells in the lung [73]. Future studies should focus on how B cell PD-L1/L2 expression affects the quantity and quality of $T_{FH,}$ T_{FR} and T_{Reg} development during infection with *Brucella* and other pathogens.

While T_{Reg} and T_{FR} promote susceptibility to *Brucella*, only T_{FR} absolutely require B cells for this effect (Figs 7A and 7F and S3H). To gain insight as to how T_{FR} impact Fo B behavior to potentially alter susceptibility to infection, we performed RNA-seq on splenic Fo B isolated from $Bcl6^{fl/fl}$ and $FoxP3^{Cre}Bcl6^{fl/fl}$ mice at two weeks post challenge, when *Brucella* burdens are similar in these strains (S9A Fig), and on Fo B from naïve animals (S10 Fig and S1 Table). When comparing the transcriptional profile of Fo B from infected $Bcl6^{fl/fl}$ and $FoxP3^{Cre}Bcl6^{fl/fl}$

mice, 401 genes were differentially regulated. Interestingly, only ~5% of the genes differentially regulated when comparing Fo B obtained from infected *Bcl6*$^{fl/fl}$ and FoxP3^{Cre}*Bcl6*$^{fl/f}$ mice were also differentially regulated when comparing Fo B from naïve *Bcl6*$^{fl/fl}$ and FoxP3^{Cre}*Bcl6*$^{fl/f}$ mice (S10B and S10C Fig) indicating the effect of T_{FR} on Fo B transcription is context dependent. Interestingly, RNA-seq analysis revealed decreased Fo B transcription of *Tgfb3* in *Brucella*-infected T_{FR} deficient mice (S10A Fig). As TGF-β3 production by B cells has been shown to drive expansion of T_{Reg} [74], which are deleterious to control of *Brucella* (S3 Fig), regulation of B cell TGF-β3 expression by T_{FR} could alter susceptibility to *Brucella*. We also observed decreased transcription of dual specificity phosphatase 4 (*Dusp4*) in T_{FR} deficient mice (S10A Fig). *Dusp4* is induced upon B cell activation involving both CD40 engagement and BCR signaling and promotes apoptosis via negative regulation of JNK (1/2) [75]. As CD40:CD40L interactions and BCR signaling both play a part in B cell mediated susceptibility to *Brucella* (Figs 1 and 4), the role of alteration of *Dusp4* expression in B cells by T_{FR} may warrant further study. T_{FR} deficiency also altered transcription of genes involved in splenic compartmentalization/follicular positioning (*Klf2*, *Bcl6*, *Ccr6*, *Cxcr4*, *Pdlim1*) [70,71, 76–78], and antibody production (*Tgfβ3*) [79] which aligns with the established role of T_{FR} in conditioning B cell reactions during GC responses. Changes in the positioning of Fo B could alter interactions with $CD4^+$ T cells. Thus, as B cell mediated susceptibility to *Brucella* is $CD4^+$ T cell dependent ([19] and Fig 2), in the future we will investigate whether T_{FR} alter the positioning of Fo B and the frequency and/or magnitude of interactions of Fo B with $CD4^+$ T cells.

Alternatively, T_{FR} may negatively impact the ability of non-B cell populations to effectively control infection. Due to the reciprocal regulation inherent in generation of T_{FH}, T_{FR} and GC B responses [20,32,52], B cell deficiency lowers T_{FR} proportions (Fig 4E and 4H). Therefore, B cell dependent effects of T_{FR} may arise from their dependence on B cells for generation or maintenance. In this case, T_{FR} could either act directly on B cells, or could function to alter other T- and/or non-B cell populations. Interestingly, T_{FR} deficiency in mice has been linked to upregulation of granzyme B and other cytotoxicity associated genes in T_{FH} [33], indicating that T_{FR} can modulate the function of other $CD4^+$ T cell populations.

In sum, our findings indicate B cells promote T_{FR} responses that are regulated by CD40L and PD-1 dependent mechanisms. T_{FR} in turn promote susceptibility to infection in a manner independent of the humoral response (S11 Fig). T_{FR} deficiency can enhance protection against influenza [62], but to our knowledge, this is the first report of an antibody independent effect of T_{FR} altering resistance to infection. Future studies will need to determine whether T_{FR} mediate B cell responses which in turn promote infection, or whether their deleterious effect is mediated by altering responses of non-B cell populations. Finally, investigating how B cell antigen specificity, presentation and T_{FR} induction synergize to hamper control of infection independent of the antibody response could have broad implications for rational vaccine designs which seek to optimize T_{FH} and GC B responses.

Materials and methods

Ethics statement

All mouse experiments were approved by the University of Missouri Animal Care and Use Committee (ACUC protocol 27761).

Growth conditions and bacterial strains

All experiments were performed using *Brucella melitensis* 16M obtained from Montana State University (Bozeman, MT) in biosafety level 3 (BSL-3) facilities. Bacteria were grown on *Brucella* agar (Becton Dickinson) at 37˚C/5% CO_2 before colonies were picked and cultured in

Brucella broth overnight at 37˚C in an orbital shaker. Challenge doses were approximated by measurement of optical density at 600 nm and diluted using sterile Dulbecco's Phosphate Buffered Saline (DPBS) (Thermofisher). All *in vivo* studies employed an intraperitoneal injection of $1x10^5$ CFUs of *B. melitensis* 16M in 200 μl of DPBS. The delivered dose was confirmed via plating of inoculum onto *Brucella* agar.

Mice

Animals challenged with *B. melitensis* were of mixed sex and were age (6–12 weeks) and sex matched for all experiments. Mice were maintained in individually ventilated caging under high efficiency particulate air-filtered barrier conditions with 12 hr light and dark cycles within ABSL-3 facilities at the University of Missouri. Food and water were provided to animals ad libitum. B6.129S2-*Ighm*^{tm1Cgn}/J (μMT), B6.129S7-Rag1tm1Mom/J (*Rag1*$^{-/-}$), C57BL/6-Tg (IghelMD4)4Ccg/J (MD4), B6.129X1-*H2-Ab1*^{tm1Koni}/J (*iAB*$^{fl/fl}$), C.B6-Tg(Foxp3-DTR/EGFP) 23.2Spar/Mmjax (DEREG), B6.129S(FVB)-Bcl6tm1.1Dent/J (*Bcl6*$^{fl/fl}$), CBA/CaJ, and CBA/CaHN-Btk^{XID}/J (XID) and C57BL/6J (WT) mice were obtained from the Jackson Laboratory. With the exception of XID mice and their controls (CBA/CaJ mice), all animal strains were on a C57BL/6 background. *sIgM*$^{-/-}$/*AID*$^{-/-}$ mice were a gift from Dr. Nicole Baumgarth at the University of California, Davis. *AID*$^{-/-}$ mice were originally generated at Kyoto University [80] and were bred to *sIgM*$^{-/-}$ mice at the Trudeau Institute [81]. B6.129P2(C)-Cd19tm1(cre)Cgn/J (CD19^{Cre}) and B6.Cg-Tg(Cd4-cre)1Cwi/BfluJmice (CD4^{Cre}) were a gift from Dr. Mark Daniels (University of Missouri). CD19^{Cre} animals were intercrossed with *iAB*$^{fl/fl}$ animals to generate CD19^{Cre}*iAB*$^{fl/fl}$ mice. *FoxP3*$^{Cre+/+}$*Bcl6*$^{fl/fl}$ (Bcl6FC) animals were gifted from Dr. Alexander Dent (University of Indiana). CD4^{Cre} and *FoxP3*$^{Cre+/+}$ animals were intercrossed with *Bcl6*$^{fl/fl}$ mice to generate *Cd4*^{Cre}*Bcl6*$^{fl/fl}$ and *FoxP3*$^{Cre+/+}$*Bcl6*$^{fl/fl}$ respectively. Experiments involving challenge of MD4, or CD19^{Cre}*iAB*$^{fl/fl}$ mice utilized HEL-negative or *iAB*$^{fl/fl}$ litter mates as control animals respectively. In all experiments using CD4^{Cre}*Bcl6*$^{fl/fl}$ or *FoxP3*^{Cre}*Bcl6*$^{fl/fl}$ animals, *Bcl6*$^{fl/fl}$ mice were used as controls. A description of the phenotypes of mice employed in this study are shown in Table 1.

Quantification of bacterial burden

Spleens were mechanically homogenized, serially diluted, and aliquots plated in triplicate onto *Brucella* agar as previously described [82]. Plated samples were incubated for 3–4 days at

Table 1. Mouse Strains used in this Study.

Mouse Strain	Phenotype
C57BL/6	Wild-type (WT) mice
MD4	Express BCR specific for Hen Egg Lysozyme
sIgM$^{-/-}$/*AID*$^{-/-}$	Cannot secrete IgM or class switched antibodies
XID	Defect in Bruton's tyrosine kinase
CBA/J	Control for XID mice
CD19^{Cre}*iAB*$^{fl/fl}$	Lack B cell MHCII expression
iAB$^{fl/fl}$	Control for CD19^{Cre}*iAB*$^{fl/fl}$ mice
μMT	Lack B cells
CD4^{cre}*Bcl6*$^{fl/fl}$	Lack T follicular helper cells
FoxP3^{cre}*Bcl6*$^{fl/fl}$	Lack T follicular regulatory cells
CD4^{cre}*Bcl6*$^{fl/fl}$	Control for CD4^{cre}*Bcl6*$^{fl/fl}$ and FoxP3^{cre}*Bcl6*$^{fl/fl}$ mice
DEREG	Express diphtheria toxin receptor under control of FoxP3 promoter
Rag1$^{-/-}$	Lack T and B cells

https://doi.org/10.1371/journal.ppat.1011672.t001

37˚C/5%CO_2, and colonies counted to quantify the total CFUs/tissue. For enumeration of viable intracellular B cell burdens, B cells were isolated from spleens of infected animals using positive selection with anti-CD19 magnetic bead isolation (Miltenyi Biotec). For each sample, an aliquot of spleen homogenate was used for B cell purification, and total splenic cells, total B cells harvested, and total B cells/spleen were calculated. To kill extracellular bacteria, spleen homogenates were incubated in complete medium (CM; RPMI 1640, 0.1 HEPES, 1 mM sodium pyruvate, 1 mM nonessential amino acids, and 10% fetal bovine serum [FBS]) containing 50 μg/ml gentamicin for 30 minutes. Homogenates were then washed, and the remaining isolation protocol carried out using MACs isolation buffer (PBS, pH 7.2, 0.5% BSA, and 2 mM EDTA) supplemented with 5 μg/mL gentamicin. $CD19^+$ and $CD19^-$ fractions were washed three times with DPBS and lysed in icy cold molecular grade water. Cell lysates were plated in triplicate to determine the *Brucella* burden for each fraction. Flow cytometric analysis of an aliquot of each sample was performed to confirm $CD19^+$ B cell fractions were >90% pure. For measurement of cytokines, homogenized tissues were centrifuged at 2000 X G for 5 minutes, and supernatants were filter sterilized (0.22 μm) and stored at −70˚C prior to analysis. Cytokines were measured with a Luminex (Austin, TX) MagPix instrument using Milliplex magnetic reagents according to manufacturer's instructions (MilliporeSigma, Burlington, MA). Luminex data were analyzed with Milliplex Analyst Software (MilliporeSigma).

Adoptive transfers

Spleens were collected from naïve animals and mechanically homogenized. For $CD4^+$ T cell and total B cell isolations, cells were magnetically purified using either CD4 or CD19 magnetic bead isolation kits (Miltenyi Biotec). Fo B cells were isolated from spleen using the MZ and FO B cell isolation kit (Miltenyi Biotec). Isolated lymphocytes were transferred via intravenous injection in 200 μL of DPBS into the tail vein of recipient mice one day prior to challenge with *B. melitensis*. Each animal received ~1.5 x 10^7 $CD4^+$ T cells alone, ~1.5 x 10^7 $CD4^+$ T cells in tandem with 5 x 10^7 (total B cell), or ~1.5 x 10^7 $CD4^+$ T cells in tandem with 3-5x10^7 Fo B cells. For B-1a cell transfers, cells were harvested from the peritoneal cavity and pleural space of naïve mice [83]. Cells from the peritoneum and pleural cavity were pooled and B-1a cells purified using the mouse B-1a cell isolation kit (Miltenyi Biotec). B-1a transfer groups received ~2x10^5 B-1a cells in 200 μl of PBS or ~2x10^5 B-1a cells in 200 μl of PBS concomitant with intravenous administration of $CD4^+$ T cells (1.5x10^7). The purity of sorted cell populations was confirmed to be ≥90% purity via flow cytometry. Purified $CD4^+$ T and total B cells were assessed using anti-CD4 (GK1.5 Biolegend), anti-CD3 (145–2011 Biolegend), anti-CD8 (53–6.7 eBioscience), anti-CD19 (1D3 Leinco) and/or anti-B220 (RA3-6B2 Biolegend). B-1a cell purity was determined using anti-CD19 (1D3 Leinco) and/or anti-B220 (RA3-6B2 Biolegend), anti-CD5 (53–7.3 Biolegend), and anti-CD43 (S11 Biolegend).

Passive antibody transfer

Bcl6$^{fl/fl}$ and *FoxP3*^{Cre}*Bcl6*$^{fl/fl}$ mice were challenged with *B. melitensis* and whole blood drawn via intracardial exsanguination four weeks post infection. Sera were collected by centrifuging blood samples at 10,000X G for 10 minutes at room temperature. Sera samples were stored at -80˚C until passive transfer. Anti-*Brucella* IgM and IgG were quantified via ELISA as described below. For passive transfer, sera from each individual *Bcl6*$^{fl/fl}$ or *FoxP3*^{Cre}*Bcl6*$^{fl/fl}$ sample were sterilized using a 0.22 μm filter and pooled by genotype. 200 μL from either *Bcl6*$^{fl/fl}$ or *FoxP3*^{Cre}*Bcl6*$^{fl/fl}$ pooled stock were administered i.p. to naïve *FoxP3*^{Cre}*Bcl6*$^{fl/fl}$ mice twenty-four hours prior to infection.

Anti-*Brucella* antibody ELISA

ELISA performed as previously described with minor modifications [8,84]. Briefly, 96-well high binding plates (Nunc), were coated overnight at 4˚C with 10^8 CFU equivalents of the heat killed *B*. *abortus* S19 vaccine strain (University of Wyoming) in 0.05 M carbonate/bicarbonate coating buffer (pH 9.6). For measuring total Ig levels and for the standard curve, either unlabeled rat anti-mouse IgM (5 μg/ml) or goat anti-mouse IgG (0.5 μg/ml) (Southern Biotech) were used to coat IgM or IgG ELISA plates respectively. Plates were then washed using PBS-T buffer (0.05% Tween-20 in 1x PBS) before blocking for 1 hr at room temperature using 1% BSA in PBS. Plates were washed again before addition of serially diluted serum, or serially diluted IgM/IgG (standard curve) and allowed to incubate for 2 hrs at room temperature. ELISA plates were subsequently washed, and Goat anti-mouse IgM-HRP (1:1000) or Goat anti-mouse IgG-HRP (1:4000) antibody (Southern Biotech) added before incubation for 1 hr at room temperature. Plates were washed a final time before development with TMB substrate (Invitrogen) and addition of stop solution (2N Sulfuric acid solution). Absorbance was measured at 450 nm using a SpectraMax (Molecular Devices, San Jose, CA). Standard curves with unlabeled mouse IgM or IgG were employed to estimate Ig concentrations and data are presented in Units/ml (U/ml), where 1 U/ml roughly correlates with 1 pg/ml of antibody. The limit of detection for anti-*Brucella* antibody was 30.9 U/ml for IgM, and 3.43 U/ml for IgG.

Flow cytometry

Spleens were homogenized and cell suspensions filtered through sterile 40 μm mesh following red blood cell lysis. Splenocytes were Fc blocked (2.4G2 Leinco) in fluorescence-activated cell-sorting (FACS) buffer (2% heat inactivated fetal bovine serum in DPBS) before extracellular staining with fluorochrome-conjugated mAbs: anti-CD4 (GK1.5 Biolegend), anti-CXCR5 (L138D7 Biolegend), anti-CD44 (IM7 Biolegend), anti-CD23 (B3B4 Biolegend), anti-CD19 (1D3 Biolegend) or anti-CD19 (6D5 Biolegend), anti-CD43 (S11 Biolegend), anti-CD21 (7E9 Biolegend), anti-B220 (RA3-6B2 eBioscience), anti-CD8 (53–6.7 Biolegend), anti-CD3 (145-2C11 Biolegend or BD Biosciences), anti-I-A/I-E(MHCII) (M5/114.15.2 Biolegend), anti-CD279 (PD-1) (29F.1A12 Biolegend), anti-CD278 (ICOS) (7E.17G9 BD Biosciences), anti-mu/HU GL7 antigen (GL7 Biolegend), anti-CD95 (Fas) (SA367H8 Biolegend), and eBioscience Fixable Viability Dye eFluor 780 (Invitrogen). Cells were then fixed in 4% formalin at 4˚C overnight before washing with and resuspension in FACS buffer. For intracellular staining, samples were fixed and permeabilized using the eBioscience Foxp3/Transcription Factor Staining Buffer Set (Thermofisher) for 30 minutes at room temperature following extracellular staining. Samples were then stained with anti-T-bet (4B10 Biolegend) and anti-FoxP3 (FJK.16s Invitrogen) for two hours before fixation with 4% formalin at 4˚C overnight, washing and resuspension in FACS buffer. Fluorescence was measured using a CyAn ADP High-Performance Flow Cytometer, BD LSR Fortessa X-20, or a Cytek Aurora spectral analyzer. Fluorescence Minus One (FMO) controls were utilized to identify rare or dim populations such as CXCR5 and PD-1 expressing cells (S12 Fig). Data were analyzed using FlowJo (Tree Star) software.

In vivo cell depletions

Animals were depleted of $CD4^+$ or $CD8^+$ T cells as previously described [19,85]. Briefly, animals were treated with 0.5 mg of rat anti-CD4 mAb GK1.5 (Leinco) or 0.2 mg rat anti-CD8 mAb 2.43 (Leinco) in 200 μl of DPBS i.p. one day prior to challenge. Treatment was repeated once weekly for the entirety of each study. For depletion of B cells, animals were treated with 250 μg of rat anti-CD20 mAB MB20-11 (BioXcell) in 200μl of DPBS i.p. one week prior to

challenge [86]. Anti-CD20 treatment was repeated on day 14 post infection. Control animals for both T and B cell depletions received equivalent dosages of rat or mouse IgG (Leinco or Southern Biotech) respectively. Upon euthanasia, depletion of splenic $CD4^+$ T, $CD8^+$ T, or B cell populations were confirmed to be $\geq$ 90% effective via flow cytometry. T_{Reg} were depleted in DEREG animals by administering 1 μg DTX (List Biological Laboratories) resuspended in 100 μL DPBS i.p. to each animal on day 14 and 15 post challenge [59]. WT animals were administered an identical dose of DTX as a control. Blood was collected from animals to confirm systemic depletion of $FoxP3^+CD4^+$ T cells seven days post treatment (S3A Fig).

CD40L and PD-1 blockade

WT and/or μMT animals were administered 250 μg, hamster anti-CD154 (CD40L) mAB MR-1 (BioXcell), or 250 μg of rat anti-CD279 (PD-1) mAB RMP1-14 (Leinco) in 200 μL of DPBS i.p. one day prior to the start of the study. Treatments were repeated every three days thereafter for the duration of the study based on the regimens of others [87,88]. Control animals were treated with equivalent dosages of either hamster IgG (CD40L) (Southern Biotech) or rat IgG (PD-1) (Leinco).

RNA-Seq analysis

Fo B cells were sorted from naïve or infected animals as described above, and were washed, and placed in 1 ml of RNAlater (Thermo) and stored at 4˚C overnight. The B cell purity of cells isolated from *Bcl6* and $FoxP3^{Cre}Bcl6^{fl/fl}$ averaged 93.5% and 97.4% respectively. Fo B cell ($CD23^+CD21^{lo}B220^+$) purity averaged ~85% of live $B220^+$ cells as determined by flow cytometry in both strains. Approximately $4x10^6$-$1x10^7$ Fo B were harvested from each animal. RNA was purified according to manufacturer instructions using a RNeasy Mini kit (Qiagen). Poly A enriched stranded mRNA libraries were generated, which were then sequenced on a NovaSeq 6000 (Illumina) as described elsewhere [89]. RNA-seq data were analyzed by the University of Missouri Bioinformatics Core Facility. Initial quality control of raw paired-end reads (100bp) was performed FastQC (v.0.11.8, https://www.bioinformatics.babraham.ac.uk/projects/fastqc/). Subsequently, fastp [90] with default parameters was used to remove adapter sequences and quality trim reads. Trimmed reads were aligned to the mouse genome assembly (mm39, annotation V109, Ensembl: http://useast.ensembl.org/Mus_musculus/Info/Index) and gene read count was quantified using STAR [91]. The gene counts for each sample were transformed and normalized using the variance-stabilizing transformation method implemented in the Bioconductor package DESeq2 [92] in R (v4.2.1; https://www.r-project.org/). Linear regression models within DESeq2 were used to identify differentially expressed genes between case vs. control sample sets. Final values for differential expression are log2 fold change $\geq$ 1 or $\leq$ -1 with false discovery rate $<$ 0.05 (FDR, Benjamini-Hochberg) as significant.

Statistical analysis

All comparisons of means between two groups were assessed via Student *t* test with significance set at $P \leq 0.05$. Comparisons of three or more groups were conducted using one-way ANOVA, followed by Tukey's test for correction of multiple comparisons unless otherwise noted. For all experiments, error bars represent the standard deviation of the sample mean. N values and the number of experimental repeats are provided in the figure legends. All statistical analyses were performed with Prism software (version 9.2, GraphPad) and all error bars indicate standard deviation (S.D.). Statistically significant differences are indicated as *, $P \leq 0.05$; **, $P \leq 0.01$; ***, $P \leq 0.001$; ****, $P \leq 0.0001$; and NS, not significant.

Supporting information

S1 Fig. MD4 animals have reduced anti-*Brucella* antibody levels. Total IgM and IgG levels were measured in the serum of MD4 and WT mice (n = 8–10 group) four weeks after infection with *B*. *melitensis* **(A)**. Serum anti-*Brucella* IgM **(B)** and IgG **(C)** in MD4 and WT mice (n = 5-11/group/time point) at two- and four-weeks post challenge with *B*. *melitensis*. Total B cell ($CD19^+$) numbers **(D)** were determined in the spleens of WT and MD4 mice (n = 8-10/group/time point) 1, 2, or 4 weeks after infection challenge with *B*. *melitensis*. **(E)** Splenic *Brucella* burdens four weeks post challenge of XID mice (n = 5/treatment) adoptively transferred B-1a cells or DPBS one day prior to infection. **(F-I)** Quantification of splenic $CD4^+$ T cell responses assessed via flow cytometry in *B*. *melitensis* infected animals. T-bet **(F)** and FoxP3 **(G)** were measured on $CD44^+CD4^+$ T cells in WT and μMT mice (n = 3-6/group/time point) at two weeks post infection. FoxP3 **(H)** and T-bet **(I)** were assessed on $CD44^+CD4^+$ T cells in *Rag1*$^{-/-}$ mice (n = 5-6/treatment) that received either $CD4^+$ T cells alone, or $CD4^+$ T cells in tandem with B cells, one day prior to challenge with *B*. *melitensis*. **(J)** Splenic bacterial burdens in *Rag1*$^{-/-}$ mice (n = 5/treatment) administered PBS, $CD4^+$ T cells alone, or $CD4^+$ T cells in combination with B-1a cells one day prior to *B*. *melitensis* challenge. Data in **(A-C and E-I)** are from a single experiment. Data in **(D)** are pooled from two experiments, and data in **(J)** are representative of at least two independent experiments.
(TIF)

S2 Fig. Enhanced susceptibility of $CD4^{Cre}$*Bcl6*$^{fl/fl}$ mice is $CD8^+$ T cell independent. The total number of $CD19^+$ B cells (A), germinal center B cells ($CD19^+Fas^+GL7^+$) (B), T_{Reg} ($FoxP3^+CXCR5^-CD44^+CD4^+$) (C), T_{FH} ($FoxP3^-ICOS^+CXCR5^+CD44^+CD4^+$) (D) and T_{FR} ($FoxP3^+ICOS^+CXCR5^+CD44^+CD4^+$) (E) were counted in the spleens of WT mice treated with IgG or anti-CD40L (n = 5/treatment) four weeks after infection with *B*. *melitensis*. Splenic bacterial burdens (F) in *Bcl6*$^{fl/fl}$ and $CD4^{Cre}$*Bcl6*$^{fl/fl}$ mice (n = 4-5/treatment) treated with CD8-depleting antibody or IgG as an isotype four weeks after *B*. *melitensis* infection. (G) Quantification of the percent T-bet$^+$ cells amongst activated ($CD44^+$) $CD4^+$ T cells in the spleens of *Bcl6*$^{fl/fl}$ and $CD4^{Cre}$*Bcl6*$^{fl/fl}$ animals (n = 4-5/group) four weeks post *B*. *melitensis* infection. The number of T_{Reg} ($FoxP3^+CXCR5^-CD44^+CD4^+$) (H) was determined four weeks after *B*. *melitensis* infection in the spleens of *Bcl6*$^{fl/fl}$ and $CD4^{Cre}$*Bcl6*$^{fl/fl}$ mice (n = 5-6/treatment). Data in (A-F and H) are from a single experiment, and data in (G) are representative of at least two independent experiments.
(TIF)

S3 Fig. T_{Reg} driven enhanced susceptibility to *Brucella* infection does not absolutely require B cells. WT or DEREG mice (n = 5/group) were challenged with *B*. *melitensis* and treated with DTX on D14 and D15 post infection. (A) Quantification of the percentage of T_{Reg} amongst $CD44^+CD4^+$ cells in the blood of WT and DEREG mice seven days post DTX treatment. (B) Splenic bacterial burdens in DTX-treated WT and DEREG animals. (C-D) Representative flow plots of the gating strategy (C) and quantification of (D) the percentage of B cells present in the spleens of DTX treated WT and DEREG animals four weeks post infection. (E-F) Representative flow plots (E) and quantification of the percentage of GC B cells amongst $CD19^+$ B cells (F) present in the spleens of DTX-treated WT and DEREG mice. (G) Percentage of Th1 effector cells (T-bet$^+$) amongst $CD44^+CD4^+$ T cells in WT and DEREG DTX-treated animals. (H) WT and DEREG mice (n = 6-8/treatment) treated with DTX and anti-CD20 or IgG isotype control and CFUs were measured four weeks post-infection. (I) Representative flow plots of the gating strategy to identify T_{FR} ($FoxP3^+CXCR5^+PD\text{-}1^+$) and T_{FH} ($FoxP3^-CXCR5^+PD\text{-}1^+$) within splenic tissue in infected animals. (J-K) Quantification of the

indicated populations of T_{FR} (J) and T_{FH} (K) amongst $CD44^+CD4^+$ T cells in DTX treated WT and DEREG animals. Data in (H) are combined from two independent experiments. All other data are from a single experiment.
(TIF)

S4 Fig. T_{FR} enhance susceptibility to *Brucella* independent of antibody. (A) Anti-*Brucella* IgM and IgG titers four weeks post *B. melitensis* challenge in the serum of $Bcl6^{fl/fl}$ and $FoxP3^{Cre}Bcl6^{fl/fl}$ animals (n = 10/group). **(B)** Splenic bacterial burdens of $FoxP3^{Cre}Bcl6^{fl/fl}$ mice (n = 4-5/transfer) administered pooled sera from previously infected $Bcl6^{fl/fl}$ or $FoxP3^{Cre}Bcl6^{fl/fl}$ mice one day prior to infection with *B. melitensis*. Data are from a single experiment.
(TIF)

S5 Fig. $CD4^+$ T cell responses in MD4 mice. MD4 mice or WT littermates (n = 3-5/group/timepoint) were challenged i.p. with $1x10^5$ CFUs of *B. melitensis* 16M. At one **(A-C)** or two **(D-F)** weeks post-infection flow cytometry was performed to assess CD44 expression on $CD4^+$ T cells **(A,D)**, and the expression of T-bet **(B,E)** and FoxP3 **(C,F)** on CD44 expressing $CD4^+$ T cells. Data are from a single experiment.
(TIF)

S6 Fig. B cell populations in WT and $sIgM^{-/-}/AID^{-/-}$ mice. WT or $sIgM^{-/-}/AID^{-/-}$ mice (n = 4-5/group) were challenged i.p. with $1x10^5$ CFUs of *B. melitensis* 16M. At four weeks post-infection the proportion **(A-D)** and number **(E-H)** of $CD19^+$ B cells **(A,E)**, Fo B cells ($CD23^+CD21^{lo}CD43^-CD19^+$) **(B,F)**, MZ B cells ($CD23^{lo}CD21^+CD43^-CD19^+$) **(C,G)**, and B-1 cells ($CD43^+CD19^+$) **(D,H)** was determined in the spleen. Data are from a single experiment.
(TIF)

S7 Fig. $CD4^+$ T cell responses and cytokine levels in mice lacking B cell MHCII expression. $CD19^{Cre}iAB^{fl/fl}$ or $iAB^{fl/fl}$ littermates (n = 5-6/group) were challenged i.p. with $1x10^5$ CFUs of *B. melitensis* 16M (A-C). At one-week post-infection, flow cytometry was performed to assess CD44 expression on $CD4^+$ T cells (A), and the expression of T-bet (B) and FoxP3 (C) on CD44 expressing $CD4^+$ T cells. $CD19^{Cre}iAB^{fl/fl}$ or $iAB^{fl/fl}$ littermates (n = 3-7/group) were challenged i.p. with $1x10^5$ CFUs of *B. melitensis* 16M (D-I). Two weeks after infection, colonization of the spleen was measured (D) and the splenic levels of IFN-γ (E), TNF-α (F), IL-17 (G), IL-1β (H) and IL-4 (I) were determined. Data are from a single experiment.
(TIF)

S8 Fig. Residual MHCII expression on B cells from $CD19^{Cre}iAB^{fl/fl}$ mice. $CD19^{Cre}iAB^{fl/fl}$ or $iAB^{fl/fl}$ littermates (n = 5-6/group) were challenged i.p. with $1x10^5$ CFUs of *B. melitensis* 16M **(A)**. At one and four weeks after challenge flow cytometry was performed to assess MHCII expression on $CD19^+$ B cells **(A)**. $CD19^{Cre}iAB^{fl/fl}$ mice (n = 5/group) were treated with IgG **(B)** or anti-CD4 **(C)** and challenged i.p. with $1x10^5$ CFUs of *B. melitensis* 16M. Four weeks after infection, colonization of the spleen was plotted against B cell MHCII expression in these animals in order to perform a linear regression. Data are from a single experiment.
(TIF)

S9 Fig. Cytokine levels in mice lacking T_{FH} or T_{FR}. $Bcl6^{fl/fl}$, $CD4^{Cre}Bcl6^{fl/fl}$ or $FoxP3^{Cre}Bcl6^{fl/fl}$ mice (n = 4-6/group) were challenged i.p. with $1x10^5$ CFUs of *B. melitensis* 16M **(A-F)**. Two weeks after infection, colonization of the spleen was measured **(A)** and the splenic levels of IFN-γ **(B)**, TNF-α **(C)**, IL-17 **(D)**, IL-1β **(E)** and IL-4 **(F)** were determined. Data are from a single experiment.
(TIF)

S10 Fig. T_{FR} deficiency alters Fo B transcription during *Brucella* infection. RNA-Seq of Fo B (n = 3-5/group) from T_{FR} deficient and control animals. **(A)** Z-scored heat map of selected genes differentially expressed in Fo B amongst naive $Bcl6^{fl/fl}$ and $FoxP3^{Cre}Bcl6^{fl/fl}$ and infected $Bcl6^{fl/fl}$ and $FoxP3^{Cre}Bcl6^{fl/fl}$ mice 14 days post *Brucella* challenge. **(B)** Table depicting the total number of differentially expressed genes (DE genes) detected when comparing infected and naïve $Bcl6^{fl/fl}$ and $FoxP3^{Cre}Bcl6^{fl/fl}$ animals (filtering criteria: FDR <0.05 and Log_2 FC ≥ 1 or Log_2 FC $\leq$ -1). **(C)** Venn diagram depicting the percent overlap of differentially expressed genes. Data are from a single experiment.
(TIF)

S11 Fig. Working model. (A) Ag-specific B cell presentation to splenic $CD4^+$ T cells results in inefficient $CD4^+$ T cell mediated control of infection in WT mice. T_{FR}, T_{FH}, GC B and *Brucella*-specific antibody responses develop in response to infection. **(B)** Inhibition of Fo B and $CD4^+$ T cell interaction in WT animals via treatment with CD40L blocking antibody results in enhanced control of splenic *Brucella* burdens. T_{FR}, T_{FH} and GC B responses are suppressed, suggesting one or more of these populations may enhance susceptibility during infection. **(C)** Alteration of Fo B and $CD4^+$ T cell regulation via PD-1 blockade promotes T_{FR} outgrowth and enhances susceptibility to *Brucella*. **(D)** Genetic T_{FR} specific deficiency results in reduced splenic *Brucella* loads despite similar T_{FH}, GC B cell and *Brucella*-specific antibody responses compared to control animals. This indicates T_{FR} promote susceptibility during *Brucella* infection through a mechanism that is independent of their role in shaping the humoral response to infection. Image created with Biorender.
(PNG)

S12 Fig. FMO controls. A representative plot including a sample, and fluorescence minus one (FMO) controls to show how PD-1 and CXCR5 expressing $CD4^+$ T cell populations were identified.
(TIF)

S1 Table. Table depicting expression of genes in Fo B isolated from *Brucella* infected and naïve $Bcl6^{fl/fl}$ and $FoxP3^{Cre}Bcl6^{fl/fl}$ animals (related to S10 Fig).
(XLSX)

Author Contributions

Conceptualization: Alexis S. Dadelahi, Jerod A. Skyberg.

Formal analysis: Alexis S. Dadelahi.

Funding acquisition: Jerod A. Skyberg.

Investigation: Alexis S. Dadelahi, Mostafa F. N. Abushahba, Bárbara Ponzilacqua-Silva, Catherine A. Chambers, Charles R. Moley, Carolyn A. Lacey.

Resources: Alexander L. Dent.

Writing – original draft: Alexis S. Dadelahi.

Writing – review & editing: Alexis S. Dadelahi, Jerod A. Skyberg.

References

1. Franc KA, Krecek RC, Häsler BN, Arenas-Gamboa AM. Brucellosis remains a neglected disease in the developing world: A call for interdisciplinary action. BMC Public Health. 2018; 18: 1–9. https://doi.org/10.1186/S12889-017-5016-Y PMID: 29325516

2. Pascual DW, Goodwin ZI, Bhagyaraj E, Hoffman C, Yang X. Activation of mucosal immunity as a novel therapeutic strategy for combating brucellosis. Front Microbiol. 2022; 13: 5041. https://doi.org/10.3389/fmicb.2022.1018165 PMID: 36620020

3. Hull NC, Schumaker BA. Comparisons of brucellosis between human and veterinary medicine. Infect Ecol Epidemiol. 2018. https://doi.org/10.1080/20008686.2018.1500846 PMID: 30083304

4. Goenka R, Guirnalda PD, Black SJ, Baldwin CL. B Lymphocytes provide an infection niche for intracellular bacterium *Brucella abortus*. J Infect Dis. 2012; 206: 91–8. https://doi.org/10.1093/infdis/jis310 PMID: 22561364

5. Godfroid J, Cloeckaert A, Liautard JP, Kohler S, Fretin D, Walravens K, et al. From the discovery of the Malta fever's agent to the discovery of a marine mammal reservoir, brucellosis has continuously been a re-emerging zoonosis. Veterinary Research. 2005. pp. 313–326. https://doi.org/10.1051/vetres:2005003 PMID: 15845228

6. Kaufmann AF, Fox MD, Boyce JM, Anderson DC, Potter ME, Martone WJ, et al. Airborne spread of brucellosis. Ann N Y Acad Sci. 1980; 353: 105–114. https://doi.org/10.1111/j.1749-6632.1980.tb18912.x PMID: 6939379

7. Grillá MJ, Blasco JM, Gorvel JP, Moriyán I, Moreno E. What have we learned from brucellosis in the mouse model? Veterinary Research. 2012. https://doi.org/10.1186/1297-9716-43-29 PMID: 22500859

8. Murphy EA, Sathiyaseelan J, Parent MA, Zou B, Baldwin CL. Interferon-γ is crucial for surviving a *Brucella abortus* infection in both resistant C57BL/6 and susceptible BALB/c mice. Immunology. 2001; 103: 511–518. https://doi.org/10.1046/j.1365-2567.2001.01258.x PMID: 11529943

9. Skyberg JA, Thornburg T, Kochetkova I, Layton W, Callis G, Rollins MF, et al. IFN-γ-deficient mice develop IL-1-dependent cutaneous and musculoskeletal inflammation during experimental brucellosis. J Leukoc Biol. 2012; 92: 375–387. https://doi.org/10.1189/jlb.1211626 PMID: 22636321

10. Goenka R, Parent MA, Elzer PH, Baldwin CL. B Cell–deficient mice display markedly enhanced resistance to the intracellular bacterium *Brucella abortus*. J Infect Dis. 2011; 203: 1136–1146. https://doi.org/10.1093/infdis/jiq171 PMID: 21451002

11. Durward-Diioia M, Harms J, Khan M, Hall C, Smith JA, Splitter GA. CD8+ T cell exhaustion, suppressed gamma interferon production, and delayed memory response induced by chronic *Brucella melitensis* infection. Infect Immun. 2015; 83: 4759–71. https://doi.org/10.1128/IAI.01184-15 PMID: 26416901

12. Hanot Mambres D, Machelart A, Potemberg G, De Trez C, Ryffel B, Letesson J-J, et al. Identification of immune effectors essential to the control of primary and secondary intranasal infection with *Brucella melitensis* in mice. J Immunol. 2016; 196: 3780–3793. https://doi.org/10.4049/jimmunol.1502265 PMID: 27036913

13. Vitry M-A, De Trez C, Goriely S, Dumoutier L, Akira S, Ryffel B, et al. Crucial role of gamma interferon-producing CD4+ Th1 cells but dispensable function of CD8+ T cell, B cell, Th2, and Th17 responses in the control of *Brucella melitensis* infection in mice. Infect Immun. 2012; 80: 4271–80. https://doi.org/10.1128/IAI.00761-12 PMID: 23006848

14. Clapp B, Yang X, Thornburg T, Walters N, Pascual DW. Nasal vaccination stimulates CD8+ T cells for potent protection against mucosal *Brucella melitensis* challenge. Immunol Cell Biol. 2016; 94: 496–508. https://doi.org/10.1038/icb.2016.5 PMID: 26752510

15. Clapp B, Skyberg JA, Yang X, Thornburg T, Walters N, Pascual DW. Protective live oral brucellosis vaccines stimulate Th1 and Th17 cell responses. Infect Immun. 2011; 79: 4165–4174. https://doi.org/10.1128/IAI.05080-11 PMID: 21768283

16. EJ Y. Human brucellosis. Rev Infect Dis. 1983; 5. https://doi.org/10.1093/CLINIDS/5.5.821 PMID: 6356268

17. Durward M, Radhakrishnan G, Harms J, Bareiss C, Magnani D, Splitter GA. Active evasion of CTL mediated killing and low quality responding CD8+ T cells contribute to persistence of brucellosis. PLoS One. 2012; 7: e34925. https://doi.org/10.1371/journal.pone.0034925 PMID: 22558103

18. Vitry M-A, Hanot Mambres D, De Trez C, Akira S, Ryffel B, Letesson J-J, et al. Humoral immunity and CD4 + Th1 cells are both necessary for a fully protective immune response upon secondary infection with *Brucella melitensis*. J Immunol. 2014; 192: 3740–3752. https://doi.org/10.4049/jimmunol.1302561 PMID: 24646742

19. Dadelahi AS, Lacey CA, Chambers CA, Ponzilacqua-Silva B, Skyberg JA. B cells inhibit CD4+ T cell mediated immunity to *Brucella* infection in a major histocompatibility complex class ii-dependent manner. Infect Immun. 2020; 88. https://doi.org/10.1128/IAI.00075-20 PMID: 32071068

20. Crotty S. T follicular helper cell biology: A decade of discovery and diseases. Immunity. 2019; 50: 1132–1148. https://doi.org/10.1016/j.immuni.2019.04.011 PMID: 31117010

21. Sage PT, Sharpe AH. T follicular regulatory cells. Immunol Rev. 2016; 271: 246–259. https://doi.org/10.1111/imr.12411 PMID: 27088919

22. Chung Y, Tanaka S, Chu F, Nurieva RI, Martinez GJ, Rawal S, et al. Follicular regulatory T cells expressing Foxp3 and Bcl-6 suppress germinal center reactions. Nat Med. 2011; 17: 983–988. https://doi.org/10.1038/nm.2426 PMID: 21785430

23. Sage PT, Paterson AM, Lovitch SB, Sharpe AH. The coinhibitory receptor CTLA-4 controls B cell responses by modulating T follicular helper, T follicular regulatory, and T regulatory cells. Immunity. 2014; 41: 1026–1039. https://doi.org/10.1016/j.immuni.2014.12.005 PMID: 25526313

24. Linterman MA, Pierson W, Lee SK, Kallies A, Kawamoto S, Rayner TF, et al. Foxp3+ follicular regulatory T cells control the germinal center response. Nat Med. 2011; 17: 975–982. https://doi.org/10.1038/nm.2425 PMID: 21785433

25. Wing JB, Kitagawa Y, Locci M, Hume H, Tay C, Morita T, et al. A distinct subpopulation of CD25− T-follicular regulatory cells localizes in the germinal centers. Proc Natl Acad Sci U S A. 2017; 114: E6400–E6409. https://doi.org/10.1073/pnas.1705551114 PMID: 28698369

26. Wollenberg I, Agua-Doce A, Hernández A, Almeida C, Oliveira VG, Faro J, et al. Regulation of the germinal center reaction by Foxp3 + follicular regulatory T cells. J Immunol. 2011; 187: 4553–4560. https://doi.org/10.4049/jimmunol.1101328 PMID: 21984700

27. Sage PT, Francisco LM, Carman C V., Sharpe AH. The receptor PD-1 controls follicular regulatory T cells in the lymph nodes and blood. Nat Immunol. 2013; 14: 152–161. https://doi.org/10.1038/ni.2496 PMID: 23242415

28. Clement RL, Daccache J, Mohammed MT, Diallo A, Blazar BR, Kuchroo VK, et al. Follicular regulatory T cells control humoral and allergic immunity by restraining early B cell responses. Nat Immunol. 2019; 20: 1360. https://doi.org/10.1038/s41590-019-0472-4 PMID: 31477921

29. Wu H, Chen Y, Liu H, Xu LL, Teuscher P, Wang S, et al. Follicular regulatory T cells repress cytokine production by follicular helper T cells and optimize IgG responses in mice. Eur J Immunol. 2016; 46: 1152–1161. https://doi.org/10.1002/eji.201546094 PMID: 26887860

30. Laidlaw BJ, Lu Y, Amezquita RA, Weinstein JS, Vander Heiden JA, Gupta NT, et al. Interleukin-10 from CD4+ follicular regulatory T cells promotes the germinal center response. Sci Immunol. 2017; 2. https://doi.org/10.1126/sciimmunol.aan4767 PMID: 29054998

31. Sayin I, Radtke AJ, Vella LA, Jin W, Wherry EJ, Buggert M, et al. Spatial distribution and function of T follicular regulatory cells in human lymph nodes. J Exp Med. 2018; 215: 1531–1542. https://doi.org/10.1084/jem.20171940 PMID: 29769249

32. Xie MM, Dent AL. Unexpected help: follicular regulatory T cells in the germinal center. Front Immunol. 2018; 9: 1536. https://doi.org/10.3389/fimmu.2018.01536 PMID: 30013575

33. Xie MM, Fang S, Chen Q, Liu H, Wan J, Dent AL. Follicular regulatory T cells inhibit the development of granzyme B-expressing follicular helper T cells. JCI insight. 2019;4. https://doi.org/10.1172/jci.insight.128076 PMID: 31434804

34. Sage PT, Sharpe AH. T follicular regulatory Cells in the regulation of B cell responses. Trends Immunol. 2015; 36: 410. https://doi.org/10.1016/j.it.2015.05.005 PMID: 26091728

35. Barroso M, Tucker H, Drake L, Nichol K, Drake JR. Antigen-B Cell Receptor complexes associate with intracellular major histocompatibility complex (MHC) class II molecules. J Biol Chem. 2015; 290: 27101. https://doi.org/10.1074/jbc.M115.649582 PMID: 26400081

36. Goodnow CC, Crosbie J, Adelstein S, Lavoie TB, Smith-Gill SJ, Brink RA, et al. Altered immunoglobulin expression and functional silencing of self-reactive B lymphocytes in transgenic mice. Nature. 1988; 334: 676–682. https://doi.org/10.1038/334676a0 PMID: 3261841

37. Wieland A, Shashidharamurthy R, Kamphorst AO, Han JH, Aubert RD, Choudhury BP, et al. Antibody effector functions mediated by Fcγ-receptors are compromised during persistent viral infection. Immunity. 2015; 42: 367–378. https://doi.org/10.1016/j.immuni.2015.01.009 PMID: 25680276

38. Kumazaki K, Tirosh B, Maehr R, Boes M, Honjo T, Ploegh HL. AID−/−μs−/− Mice are agammaglobulinemic and fail to maintain B220−CD138+ plasma cells. J Immunol. 2007; 178: 2192–2203. https://doi.org/10.4049/JIMMUNOL.178.4.2192 PMID: 17277124

39. Sharma S, Orlowski G, Song W. Btk regulates B cell receptor-mediated antigen processing and presentation by controlling actin cytoskeleton dynamics in B cells. J Immunol. 2009; 182: 329–339. https://doi.org/10.4049/jimmunol.182.1.329 PMID: 19109164

40. Khan WN, Alt FW, Gerstein RM, Malynn BA, Larsson I, Rathbun G, et al. Defective B cell development and function in Btk-deficient mice. Immunity. 1995; 3: 283–299. https://doi.org/10.1016/1074-7613(95)90114-0 PMID: 7552994

41. Smith FL, Baumgarth N. B-1 cell responses to infections. Curr Opin Immunol. 2019; 57: 23. https://doi.org/10.1016/j.coi.2018.12.001 PMID: 30685692

42. Serrán MG, Boari JT, Vernengo FF, Beccaría CG, Ramello MC, Bermejo DA, et al. Unconventional pro-inflammatory CD4+ T cell response in B cell-deficient mice infected with *Trypanosoma cruzi*. Front Immunol. 2017;8. https://doi.org/10.3389/fimmu.2017.01548 PMID: 29209313

43. Breitfeld D, Ohl L, Kremmer E, Ellwart J, Sallusto F, Lipp M, et al. Follicular B helper T cells express CXC chemokine receptor 5, localize to B cell follicles, and support immunoglobulin production. J Exp Med. 2000; 192: 1545–1551. https://doi.org/10.1084/jem.192.11.1545 PMID: 11104797

44. Kim CH, Rott LS, Clark-Lewis I, Campbell DJ, Wu L, Butcher EC. Subspecialization of CXCR5+ T cells: B helper activity is focused in a germinal center-localized subset of CXCR5+ T cells. J Exp Med. 2001; 193: 1373–1381. https://doi.org/10.1084/jem.193.12.1373 PMID: 11413192

45. Stebegg M, Kumar SD, Silva-Cayetano A, Fonseca VR, Linterman MA, Graca L. Regulation of the germinal center response. Front Immunol. 2018; 9: 2469. https://doi.org/10.3389/fimmu.2018.02469 PMID: 30410492

46. Awe O, Hufford MM, Wu H, Pham D, Chang H-C, Jabeen R, et al. PU.1 expression in T follicular helper cells limits CD40L-dependent germinal center B cell development. J Immunol. 2015; 195: 3705–3715. https://doi.org/10.4049/jimmunol.1500780 PMID: 26363052

47. Elgueta R, Benson MJ, De Vries VC, Wasiuk A, Guo Y, Noelle RJ. Molecular mechanism and function of CD40/CD40L engagement in the immune system. Immunol Rev. 2009; 229: 152–172. https://doi.org/10.1111/j.1600-065X.2009.00782.x PMID: 19426221

48. Nurieva RI, Chung Y, Martinez GJ, Yang XO, Tanaka S, Matskevitch TD, et al. Bcl6 mediates the development of T follicular helper cells. Science (1979). 2009; 325: 1001–1005. https://doi.org/10.1126/science.1176676 PMID: 19628815

49. Johnston RJ, Poholek AC, DiToro D, Yusuf I, Eto D, Barnett B, et al. Bcl6 and Blimp-1 are reciprocal and antagonistic regulators of T follicular helper cell differentiation. Science. 2009; 325: 1006–1010. https://doi.org/10.1126/science.1175870 PMID: 19608860

50. Ichii H, Sakamoto A, Hatano M, Okada S, Toyama H, Taki S, et al. Role for Bcl-6 in the generation and maintenance of memory CD8 + T cells. 2002. https://doi.org/10.1038/ni802 PMID: 12021781

51. Carpenter AC, Bosselut R. Decision checkpoints in the thymus. Nat Immunol. 2010; 11: 666. https://doi.org/10.1038/ni.1887 PMID: 20644572

52. Hollister K, Kusam S, Wu H, Clegg N, Mondal A, Sawant D V., et al. Insights into the role of Bcl6 in follicular Th cells using a new conditional mutant mouse model. J Immunol. 2013; 191: 3705–3711. https://doi.org/10.4049/jimmunol.1300378 PMID: 23980208

53. Tan CL, Kuchroo JR, Sage PT, Liang D, Francisco LM, Buck J, et al. PD-1 restraint of regulatory T cell suppressive activity is critical for immune tolerance. J Exp Med. 2021;218. https://doi.org/10.1084/jem.20182232 PMID: 33045061

54. Eschweiler S, Clarke J, Ramírez-Suástegui C, Panwar B, Madrigal A, Chee SJ, et al. Intratumoral follicular regulatory T cells curtail anti-PD-1 treatment efficacy. Nat Immunol. 2021 228. 2021; 22: 1052–1063. https://doi.org/10.1038/s41590-021-00958-6 PMID: 34168370

55. Vinuesa CG, Linterman MA, Yu D, MacLennan ICM. Follicular helper T cells. Annu Rev Immunol. 2016; 34: 335–368. https://doi.org/10.1146/annurev-immunol-041015-055605 PMID: 26907215

56. Haynes NM, Allen CDC, Lesley R, Ansel KM, Killeen N, Cyster JG. Role of CXCR5 and CCR7 in follicular Th cell positioning and appearance of a programmed cell death gene-1 high germinal center-associated subpopulation. J Immunol. 2007; 179: 5099–108. https://doi.org/10.4049/jimmunol.179.8.5099 PMID: 17911595

57. Jubel JM, Barbati ZR, Burger C, Wirtz DC, Schildberg FA. The role of PD-1 in acute and chronic infection. Front Immunol. 2020; 11: 487. https://doi.org/10.3389/fimmu.2020.00487 PMID: 32265932

58. Wang J, Siffert M, Spiliotis M, Gottstein B. Repeated long-term DT application in the DEREG mouse induces a neutralizing anti-DT antibody response. J Immunol Res. 2016; 2016. https://doi.org/10.1155/2016/1450398 PMID: 28074191

59. Lahl K, Sparwasser T. In vivo depletion of FoxP3+ Tregs using the DEREG mouse model. Methods Mol Biol. 2011; 707: 157–172. https://doi.org/10.1007/978-1-61737-979-6_10 PMID: 21287334

60. Adetunji SA, Faustman DL, Adams LG, Garcia-Gonzalez DG, Hensel ME, Khalaf OH, et al. *Brucella abortus* and pregnancy in mice: Impact of chronic infection on fertility and the role of regulatory t cells in tissue colonization. Infect Immun. 2020;88. https://doi.org/10.1128/IAI.00257-20 PMID: 32690635

61. Pasquali P, Thornton AM, Vendetti S, Pistoia C, Petrucci P, Tarantino M, et al. CD4+CD25+ T regulatory cells limit effector T cells and favor the progression of brucellosis in BALB/c mice. Microbes Infect. 2010; 12: 3–10. https://doi.org/10.1016/j.micinf.2009.09.005 PMID: 19772948

62. Fu W, Liu X, Lin X, Feng H, Sun L, Li S, et al. Deficiency in T follicular regulatory cells promotes autoimmunity. J Exp Med. 2018; 215: 815. https://doi.org/10.1084/jem.20170901 PMID: 29378778

63. Xie MM, Chen Q, Liu H, Yang K, Koh B, Wu H, et al. T follicular regulatory cells and IL-10 promote food antigen–specific IgE. J Clin Invest. 2020; 130: 3820–3832. https://doi.org/10.1172/JCI132249 PMID: 32255767

64. Tsiantoulas D, Kiss M, Bartolini-Gritti B, Bergthaler A, Mallat Z, Jumaa H, et al. Secreted IgM deficiency leads to increased BCR signaling that results in abnormal splenic B cell development. Sci Rep. 2017;7. https://doi.org/10.1038/S41598-017-03688-8 PMID: 28615655

65. Parra D, Rieger AM, Li J, Zhang Y-A, Randall LM, Hunter CA, et al. Pivotal advance: peritoneal cavity B-1 B cells have phagocytic and microbicidal capacities and present phagocytosed antigen to CD4+ T cells. J Leukoc Biol. 2012; 91: 525–536. https://doi.org/10.1189/jlb.0711372 PMID: 22058420

66. Voynova E, Mahmoud T, Woods LT, Weisman GA, Ettinger R, Braley-Mullen H. Requirement for CD40/CD40L interactions for development of autoimmunity differs depending on specific checkpoint and costimulatory pathways. ImmunoHorizons. 2018; 2: 54. https://doi.org/10.4049/immunohorizons.1700069 PMID: 30607385

67. Aloulou M, Carr EJ, Gador M, Bignon A, Liblau RS, Fazilleau N, et al. Follicular regulatory T cells can be specific for the immunizing antigen and derive from naive T cells. Nat Commun. 2016 71. 2016; 7: 1–10. https://doi.org/10.1038/ncomms10579 PMID: 26818004

68. Saraiva M, O'Garra A. The regulation of IL-10 production by immune cells. Nat Rev Immunol. 2010; 10: 170–181. https://doi.org/10.1038/NRI2711 PMID: 20154735

69. Xavier MN, Winter MG, Spees AM, Nguyen K, Atluri VL, Silva TMA, et al. CD4+ T cell-derived IL-10 promotes *Brucella abortus* persistence via modulation of macrophage function. PLoS Pathog. 2013; 9: e1003454. https://doi.org/10.1371/journal.ppat.1003454 PMID: 23818855

70. Nie Y, Waite J, Brewer F, Sunshine MJ, Littman DR, Zou YR. The role of CXCR4 in maintaining peripheral B cell compartments and humoral immunity. J Exp Med. 2004; 200: 1145. https://doi.org/10.1084/jem.20041185 PMID: 15520246

71. Shi J, Hou S, Fang Q, Liu X, Liu X, Qi H. PD-1 controls follicular T helper cell positioning and function. Immunity. 2018; 49: 264–274.e4. https://doi.org/10.1016/j.immuni.2018.06.012 PMID: 30076099

72. Khan AR, Hams E, Floudas A, Sparwasser T, Weaver CT, Fallon PG. PD-L1hi B cells are critical regulators of humoral immunity. Nat Commun. 2015; 6: 5997. https://doi.org/10.1038/ncomms6997 PMID: 25609381

73. Swanson R V, Gupta A, Foreman TW, Lu L, Choreno-Parra JA, Mbandi SK, et al. Antigen-specific B cells direct T follicular-like helper cells into lymphoid follicles to mediate *Mycobacterium tuberculosis* control. Nat Immunol 2023. 2023; 1–14. https://doi.org/10.1038/s41590-023-01476-3 PMID: 37012543

74. Shah S, Qiao L. Resting B cells expand a CD4+CD25+Foxp3+ Treg population via TGF-beta3. Eur J Immunol. 2008; 38: 2488–2498. https://doi.org/10.1002/eji.200838201 PMID: 18792402

75. Rickert R. DUSP4 phosphatase puts the brakes on DLBCL. J Exp Med. 2015; 212: 598–599. https://doi.org/10.1084/jem.2125insight2 PMID: 25941318

76. Hoek KL, Gordy LE, Collins PL, Parekh V V., Aune TM, Joyce S, et al. Follicular B cell trafficking within the spleen actively restricts humoral immune responses. Immunity. 2010; 33: 254–265. https://doi.org/10.1016/j.immuni.2010.07.016 PMID: 20691614

77. Choi J, Crotty S. Bcl6-Mediated transcriptional regulation of follicular helper T cells (TFH). Trends Immunol. 2021; 42: 336. https://doi.org/10.1016/j.it.2021.02.002 PMID: 33663954

78. Elgueta R, Marks E, Nowak E, Menezes S, Benson M, Raman VS, et al. CCR6-dependent positioning of memory B cells is essential for their ability to mount a recall response to antigen. J Immunol. 2015; 194: 505. https://doi.org/10.4049/jimmunol.1401553 PMID: 25505290

79. Tsuchida Y, Sumitomo S, Ishigaki K, Suzuki A, Kochi Y, Tsuchiya H, et al. TGF-β3 inhibits antibody production by human B cells. PLoS One. 2017;12. https://doi.org/10.1371/JOURNAL.PONE.0169646 PMID: 28052118

80. Muramatsu M, Kinoshita K, Fagarasan S, Yamada S, Shinkai Y, Honjo T. Class switch recombination and hypermutation require activation-induced cytidine deaminase (AID), a potential RNA editing enzyme. Cell. 2000; 102: 553–563. https://doi.org/10.1016/s0092-8674(00)00078-7 PMID: 11007474

81. Carragher DM, Kaminski DA, Moquin A, Hartson L, Randall TD. A novel role for non-neutralizing antibodies against nucleoprotein in facilitating resistance to influenza virus. J Immunol. 2008; 181: 4168–4176. https://doi.org/10.4049/jimmunol.181.6.4168 PMID: 18768874

82. Abushahba MF, Dadelahi AS, Lemoine EL, Skyberg JA, Vyas S, Dhoble S, et al. Safe subunit green vaccines confer robust immunity and protection against mucosal *Brucella* infection in mice. Vaccines. 2023; 11:546. https://doi.org/10.3390/VACCINES11030546 PMID: 36992130

83. Yenson V, Baumgarth N. Purification and immune phenotyping of B-1 Cells from body cavities of mice. Humana Press, New York, NY; 2014:17–34. https://doi.org/10.1007/978-1-4939-1161-5_2 PMID: 25015270

84. Ledbetter L, Cherla R, Chambers C, Zhang Y, Zhang G. Eosinophils affect antibody isotype switching and may partially contribute to early vaccine-induced immunity against C*oxiella burnetii*. Infect Immun. 2019;87. https://doi.org/10.1128/IAI.00376-19 PMID: 31427447

85. Grčevicgrčevic D, Lee S-K, Marušic AM, Lorenzo JA. Depletion of CD4 and CD8 T Lymphocytes in mice in vivo enhances 1,25-Dihydroxyvitamin D3-stimulated osteoclast-like cell formation in vitro by a mechanism that is dependent on prostaglandin Ssynthesis. J Immunol. 2000; 165: 4231–4238. https://doi.org/10.4049/JIMMUNOL.165.8.4231 PMID: 11035056

86. Hamaguchi Y, Uchida J, Cain DW, Venturi GM, Poe JC, Haas KM, et al. The peritoneal cavity provides a protective niche for B1 and conventional B lymphocytes during anti-CD20 immunotherapy in mice. J Immunol. 2005; 174: 4389–4399. https://doi.org/10.4049/jimmunol.174.7.4389 PMID: 15778404

87. Husaini Y, Tsai VWW, Manandhar R, Zhang HP, Lee-Ng KKM, Lebhar H, et al. Growth differentiation factor-15 slows the growth of murine prostate cancer by stimulating tumor immunity. PLoS One. 2020;15. https://doi.org/10.1371/journal.pone.0233846 PMID: 32502202

88. Wiley JA, Harmsen AG. CD40 ligand is required for resolution of *Pneumocystis carinii* pneumonia in mice. J Immunol. 1995; 155: 3525–3529. https://doi.org/10.4049/JIMMUNOL.155.7.3525

89. Moley CR, Chambers CA, Dadelahi AS, Ponzilacqua-Silva B, Abushahba MFN, Lacey CA, et al. Innate lymphoid cells and interferons limit neurologic and articular complications of brucellosis. Am J Pathol. 2023;0. https://doi.org/10.1016/j.ajpath.2023.05.006 PMID: 37263343

90. Chen S, Zhou Y, Chen Y, Gu J. fastp: an ultra-fast all-in-one FASTQ preprocessor. Bioinformatics. 2018; 34: i884–i890. https://doi.org/10.1093/bioinformatics/bty560 PMID: 30423086

91. Dobin A, Davis CA, Schlesinger F, Drenkow J, Zaleski C, Jha S, et al. STAR: ultrafast universal RNA-seq aligner. Bioinformatics. 2013; 29: 15–21. https://doi.org/10.1093/bioinformatics/bts635 PMID: 23104886

92. Love MI, Huber W, Anders S. Moderated estimation of fold change and dispersion for RNA-seq data with DESeq2. Genome Biol. 2014;15. https://doi.org/10.1186/s13059-014-0550-8 PMID: 25516281